

REPORT NO. 3772  
COPY NO. 6

FINAL REPORT

# A TAPERED-LINE, 3-DB COUPLER

RESEARCH LABORATORIES DIVISION

Bendix

Report No. 3772

# **A TAPERED-LINE 3-DB COUPLER**

## **Final Report**

**June 13, 1966 to November 13, 1966**

**Contract N123 (62738) 56114A**

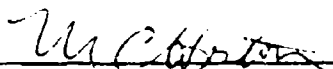
Prepared by  
C. P. Tresselt

The Bendix Corporation  
Research Laboratories Division  
Southfield, Michigan 48075

For

U. S. Naval Ordnance Laboratory  
Corona, California

Approved by:

  
M. C. Horton, Head  
Microwave Technology and Communications Department

## TABLE OF CONTENTS

	<u>Page</u>
SECTION 1 - INTRODUCTION	1
1.1 General	1
1.2 Discussion of the Design Concept	1
SECTION 2 - SYNTHESIS CONSIDERATIONS	4
2.1 Analysis of Nonuniform Line Coupler Performance	4
2.2 Monotonic $p(u)$ Couplers	6
2.3 Couplers with Periodic Zeros in $p(u)$	8
2.4 Synthesis of the 800-11,000 MHz Coupler	16
2.5 Synthesis of a 390-11,000 MHz Coupler	18
SECTION 3 - CONSTRUCTION OF THE 800-11,000 MHz COUPLER	23
3.1 Determination of Stripline Coupling Parameters	23
3.2 Layout of the Coupler	25
3.3 Construction Details	27
SECTION 4 - OPTIMIZATION OF THE 800-11,000 MHz DESIGN	30
4.1 Modification of the Center Shim	30
4.2 Suggested Design Improvement	31
4.3 Measured Coupler Performance	31
SECTION 5 - CONCLUSIONS	41
SECTION 6 - REFERENCES	43

# LIST OF ILLUSTRATIONS

<u>Figure No.</u>	<u>Title</u>	<u>Page</u>
1	First-Order Coupling Characteristics	6
2	P(u) Versus u for Several Monotonic P(u) Couplers	7
3	First-Order Response of the Couplers Described in Figure 2	7
4	Plot of $P(u) = -\frac{1}{\pi} \frac{\sin^2 u/2}{u/2}$	10
5	Frequency Response of Various Truncations of $p(u) = \frac{\sin^2 u/2}{u/2}$	10
6	Response of a Typical Periodic P(u) Coupler	12
7	Physical Coupling Versus Distance for a Tapered- Line Coupler and a Stepped-Coupler Which Provide Essentially Identical Coupling Versus Frequency Performance	15
8	Equal Ripple (800 MHz-11,256 MHz) Coupler	18
9	Stripline Parameter Test Fixture	24
10	Three-Layer Stripline Coupling Parameters	25
11	Stripline Board	26
12	800-11,000 MHz Coupler with Precision Test Loads	28
13	Predistorted Coupler Response Characteristic	32
14	Comparison Between the Flat P(u) and the Predistorted PΔ(u) Characteristics	32
15	Isolation, Transmission, and Coupling at L-Band: Input at Port 1	36
16	Isolation, Transmission, and Coupling at S-Band: Input at Port 1	36
17	Isolation, Transmission, and Coupling at C-Band: Input at Port 1	37
18	Isolation, Transmission, and Coupling at X-Band: Input at Port 1	37
19	Isolation, Transmission, and Coupling at L-Band: Input at Port 3	38
20	Isolation, Transmission, and Coupling at S-Band: Input at Port 3	38
21	Isolation, Transmission, and Coupling at C-Band: Input at Port 3	39
22	Isolation, Transmission, and Coupling at X-Band: Input at Port 3	39
23	Coupler VSWR	40
24	Final Phase Measurement Setup	40
25	Phase Deviation of Coupler Outputs from 90°	40

LIST OF TABLES

<u>Table No.</u>	<u>Title</u>	<u>Page</u>
1	UHF Performance of Coupler	33

## SECTION 1

### INTRODUCTION

#### 1.1 GENERAL

This report describes the design and fabrication of a wideband high-isolation 90 degree coupler employing tapered-line techniques. The effort was carried out under Contract N123(62738)5611A. The performance requirements of the coupler are as follows:

Frequency:	390-11,000 MHz desired 800-11,000 MHz acceptable alternate
VSWR:	1.3 db or less
Isolation:	25 db or greater
Insertion Loss:	1 db or less
Difference of Outputs: (Coupled versus Direct)	1 db or less
Phase:	90 deg $\pm$ 3 deg

It was decided to realize the 800-11,000 MHz alternate bandwidth, while providing theoretical information on the 390-11,000 MHz design. The coupler that was constructed and delivered on this program is described in detail in Section 3. The unit meets a majority of the design goals, demonstrating the usefulness of the tapering technique.

#### 1.2 DISCUSSION OF THE DESIGN CONCEPT

It is possible to obtain multi-octave bandwidth from a single coupler that employs several cascaded quarter-wavelength sections of uniformly coupled line. The use of a symmetric structure guarantees 90 degrees relative phase lead of the coupled port with respect to the transmitted port at all frequencies. Cristal and Young [1] present tables of coupling coefficients required to produce equal-ripple response for the third- through ninth-order designs, and include a comprehensive bibliography covering the historic development of this form of coupler. Tight coupling normally is required in at least one of the sections of a broad-band design. This condition has been alleviated to some extent by the application of tandem interconnection [2].

Unfortunately, the spread in coupling values required in adjacent quarter-wave sections, with or without tandem interconnection, is large enough to produce substantial differences in physical line dimensions. The abrupt transition regions between adjacent sections exhibit reactive discontinuities which degrade coupler directivity, particularly at the

higher microwave frequencies. Some compensation for these effects can be achieved by using tuning screws in the junction regions, or, if a dielectric stripline is involved, by using suitably placed capacitive tuning tabs. In general, however, these techniques have not proved very useful above C-band.

This report describes a design that eliminates the abrupt interconnections between coupled sections. The coupling coefficient is gradually tapered from loose to tight coupling (in the center) and then back to loose in a symmetrical manner to preserve the 90-degree character of the design. The familiar condition that  $\sqrt{Z_{0e} \cdot Z_{0o}} = 1$  must be observed throughout the coupler length to insure that the port adjacent to the transmitted port remains isolated.

Stepped-impedance couplers are a sub-class of tapered-line designs. In stepped-impedance devices, coupling is assumed to change abruptly between quarter-wave sections, whereas, in practice, a finite length is required to effect the desired change. The coupling versus distance characteristic present in a stepped coupler is thus tapered. This distinction may be largely neglected for couplers covering UHF and the lower microwave frequencies. However, in multi-octave designs covering frequencies through X-band, transition regions occupy a significant fraction of coupler length due to the shortness of the quarter-wave sections involved. Consider, for example, the stepped-impedance tandem coupler covering the 1 to 8 GHz band described by Shelton [2]. The transition regions associated with the center quarter-wavelength section of this design occupy at least one-third of the center section. The distributed nature of such transitions usually dictates the use of an empirical procedure to determine the best transition shape and location along the axis of the coupler. Misadjustments are readily apparent in the frequency domain since these two transitions provide the largest-amplitude Fourier contribution to the overall coupling versus frequency characteristic [2].

The nonuniform line couplers treated are tapered gradually enough to permit usage without modification of physical coupling data based on infinitely long, uniformly-coupled line calculations. This has the practical advantage of allowing the geometry of the coupler to be completely specified without the uncertainty associated with the transition regions of stepped coupler designs.

The primary motivation for investigation of tapered-line designs, however, has been the promise of higher directivity. The reactive discontinuities experienced in stepped designs result from non-propagating higher-order modes present in the vicinity of the transitions. While it is true that such evanescent modes will, to some extent, also be excited along the length of the tapered-line geometry, the amplitude of such modes decreases as the taper employed becomes more gradual with respect to wavelength. The equal-ripple tapered-line coupler described in Section 2.3 utilizes essentially a full quarter-wavelength to taper between coupling levels for which an abrupt transition is required in the

comparable stepped-coupler model. Directivity is not amenable to theoretical calculation in either the stepped or tapered cases, since a mathematical description is not available for the modes involved in practical line geometries of interest. For this reason an experimental investigation is indicated.



## SECTION 2 SYNTHESIS CONSIDERATIONS

### 2.1 ANALYSIS OF NONUNIFORM LINE COUPLER PERFORMANCE

Generalized coupler theory can be developed with the aid of the transmission-line analogy [1]. A nonuniform transmission line is postulated whose characteristic impedance curve equals the even-mode impedance curve of the coupler to be analyzed. Under these conditions, the reflection coefficient of the transmission line is equal in magnitude and phase to the coupled-arm response of the coupler.

The analysis and synthesis of nonuniform line devices is complicated by the fact that exact closed-form solutions have not been developed [3,4]. Analysis and synthesis can, however, be performed directly by using a loose-coupling approximation. As will be shown later, such results can be modified to cover tighter coupling without resorting to open-form (series) solutions.

Under the assumption of loose coupling, one can show with the aid of the transmission line analogy that coupling,  $C$ , at frequency,  $\omega$ , is given by [3]

$$C(\omega) = \int_0^d e^{-2j\omega x/v} p(x) dx, \quad (1)$$

where  $d$  is the overall coupler length,  $v$  is the velocity of propagation in the medium of interest, and

$$p(x) = \frac{1}{2} \frac{d}{dx} \ln Z_{oe}(x). \quad (2)$$

The quantity  $p(x)$  is the reflection coefficient distribution which is related by equation (2) to the even-mode impedance-versus-distance characteristic of the coupler. The coupling, as given by equation (1), is the Fourier transform of  $p(x)$ . Synthesis can thus be performed directly in the first-order approximation by application of an inverse Fourier transformation.

Second-order coupling theory can be obtained with the aid of the transmission line analogy from Youla's equation (66) [4]. The coupler is matched at its input and output so that  $\Gamma_g = \Gamma_L = 0$  for the analogous line. Furthermore, the generator and load impedances are equal, so that Youla's equation (66) becomes, in the terminology of this report,

$$C(\omega) = \frac{\left| \int_0^d e^{-j \frac{2\omega x}{v}} p(x) dx \right|}{\sqrt{1 + \left| \int_0^d e^{-j \frac{2\omega x}{v}} n(x) dx \right|^2}} \quad (3)$$

A similarity exists between first- and second-order theory, since the same integral expression appears in both solutions. For small values of coupling, the second-order expression reduces to first-order theory. For tighter values of coupling, second-order theory indicates that larger values of  $p(x)$  are required for a given coupling level than are indicated by first-order theory. Flat coupling over broad frequency bands is of primary concern. If a  $p(x)$  characteristic produces a flat first-order response, the coupling will remain flat in the second-order theory at a lower mean level, as indicated by equation (3).

Youla [4] presents an exact description of nonuniform line performance in terms of a Volterra integral equation of a type which may always be solved by successive iterations, the resulting series being absolutely and uniformly convergent under broad conditions. The number of iterations required depends on the mean level of coupling and the bandwidth. Unfortunately, a compact synthesis formula corresponding to higher-order theory has not been found.

Further insight into the design problem can be obtained from first-order considerations. Because the even-mode impedance of the coupler is symmetrical about the coupler center, the derivative of the logarithm of this curve will be odd, as shown in Figure 1(a). It is convenient to shift axis in the first-order integral to take advantage of this fact, obtaining thereby,

$$C(\omega) = -j e^{-j \frac{\omega}{v} d} \int_{-\frac{d}{2}}^{\frac{d}{2}} \sin 2 \frac{\omega}{v} u \cdot p(u) du \quad (4)$$

where

$$p(u) = \frac{1}{2} \frac{d}{du} \ln Z_{oe}(u). \quad (5)$$

The magnitude and phase of  $C(\omega)$ , corresponding to  $p(u)$  in Figure 1(a), are shown in Figure 1(b). By assuming a desired magnitude-versus-frequency

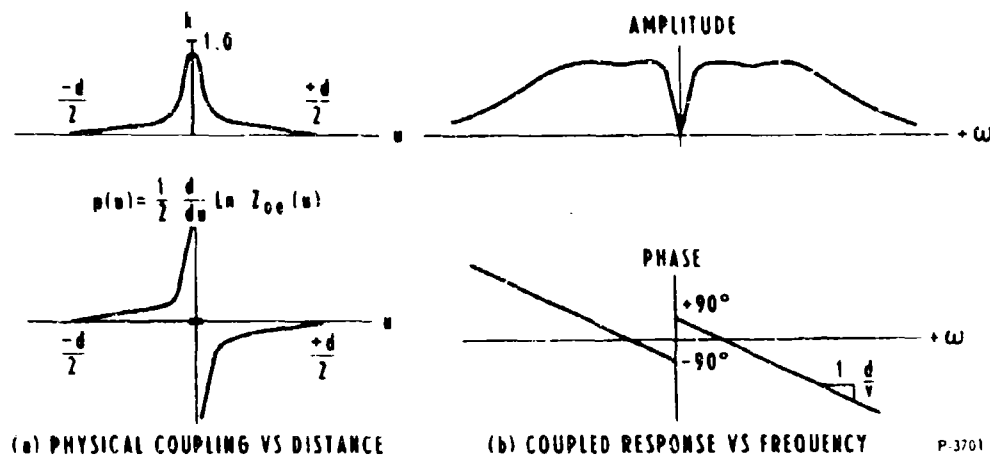


Figure 1 - First-Order Coupling Characteristics

characteristic and using phase as shown, one can, by inverse Fourier transformation, obtain the required function of coupling versus distance. A Scientific-Atlanta CF 1 Fourier integral computer has been used to perform this transformation.

## 2.2 MONOTONIC $p(u)$ COUPLERS

It is worthwhile, for purposes of comparison, to describe a class of couplers which were investigated during early studies of tapered couplers. This class possesses a monotonically increasing  $p(u)$  characteristic along the length of the coupler, as illustrated in Figure 1. Pertinent information about the approximation problem for this type of coupler can be obtained by consideration of an impedance-versus-distance curve that has been found integrable in closed form. Here, it is convenient to use the first-order theory of equation (4). Let the coupler length,  $d$ , be two units long, and let  $p(u)$  be given by

$$\begin{aligned} p(u) &= \frac{-M(1+u)}{2u}, & -1 \leq u < 0 \\ p(u) &= \frac{-M(1-u)}{2u}, & 0 < u \leq 1 \end{aligned} \quad (6)$$

This characteristic is shown in Figure 2 for  $M = 0.201$ . The magnitude of  $p(u)$  goes to  $\infty$  as  $u$  approaches zero from either side. Under these conditions, direct substitution of equation (6) into (4) leads to the result that

$$C(\theta) = jM e^{-j\theta} \left[ S_1(\theta) + \frac{1}{\theta} (\cos \theta - 1) \right], \quad (7)$$

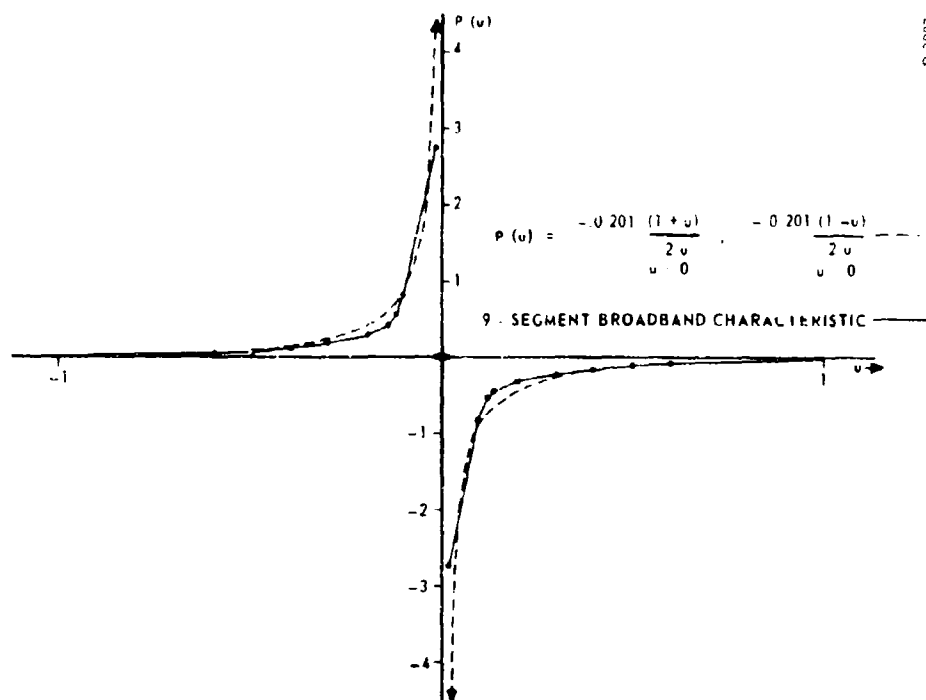


Figure 2 -  $P(u)$  Versus  $u$  for Several Monotonic  $P(u)$  Couplers

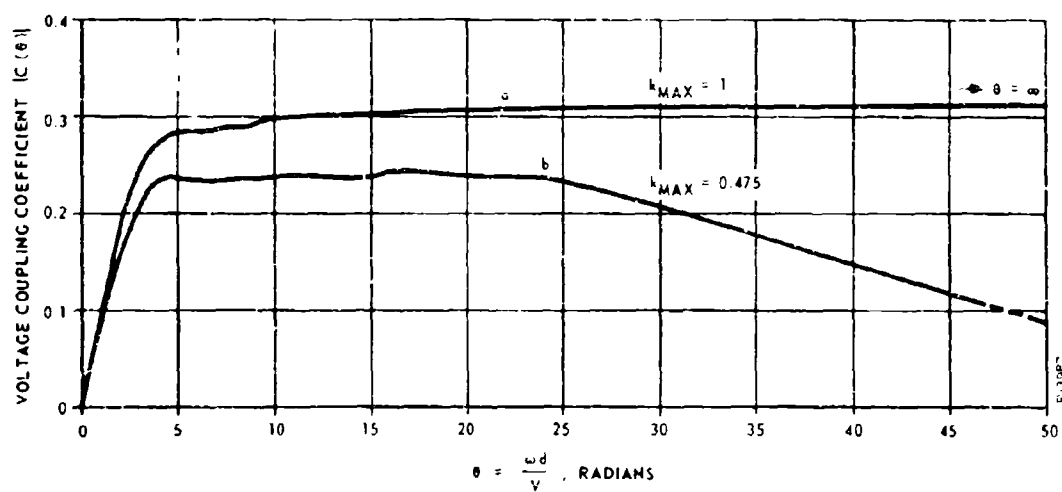


Figure 3 - First-Order Response of the Couplers Described in Figure 2

where:

$$\theta = \frac{2\pi}{v}$$

Response of this coupler for  $M = 0.201$  is plotted in Figure 3(a). The choice of  $M = 0.201$  provides a maximum coupling level  $C(\theta)_{\max} = 0.3161$ , which is -10 db. Note that coupling rises monotonically with increasing frequency and that coupling is relatively flat for  $\theta > 10$ .

Equations (5) and (6) require that  $Z_{oe} = \infty$  at the coupler center. This is not realizable in practice, since the coupling coefficient,

$$k(u) = \frac{Z_{oe}^2(u) - 1}{Z_{oe}^2(u) + 1}, \quad (8)$$

must be unity at coupler center. Simple truncation of the  $p(u)$  characteristic defined by equation (6) results in a coupling characteristic which droops severely with frequency. An iterative technique can be employed to improve such an undesirable response. A curve expressing the difference between a flat coupling level and the given coupler response is formed over the frequency interval in which flat response is desired. Fourier analysis of this error curve will give a set of  $p(u)$  values which can be added to the original  $p(u)$  characteristic to correct the discrepancy between responses. The response achieved by one particular set of iterations is shown in curve b in Figure 3. This characteristic corresponds to the  $p(u)$  curve made up of nine straight-line segments shown in Figure 2. Straight-line segments were used throughout the iterative procedure to minimize the effort required in integrating  $p(u)$  to obtain actual coupling coefficients. (A maximum coupling value of  $k = 0.475$  is required in the center of the coupler.)

One characteristic inherent in the monotonic  $p(u)$  type of coupler is the relatively slow dropoff in response at high frequencies. If this response is forced to fall off more rapidly in the correction procedure, a nonmonotonic  $p(u)$  function will be produced. The monotonically increasing  $p(u)$  coupler was the first tapered design to be investigated because of its relatively smooth coupling characteristic,  $k(u)$ . This type of coupler is not the best from a mean-coupling bandwidth standpoint as discussed below; however, in moderate bandwidth form, it should prove to be quite valuable as an instrumentation coupler.

### 2.3 COUPLERS WITH PERIODIC ZEROS IN $p(u)$

A coupling-versus-frequency characteristic which would remain flat out to some cutoff frequency, beyond which coupling would rapidly drop to zero, would be highly desirable. All the available coupling-bandwidth product would then be employed usefully. One can show, by using first-

order coupling theory described earlier in an inverse Fourier transformation sense, that a  $p(u)$  distribution given by

$$p(u) = -\frac{1}{\pi} \frac{\sin^2 u/2}{u/2} \quad (9)$$

will provide a first-order mean-coupling level of 1.0 over the frequency range from 0 to 1 radian/second. This function is shown in Figure 4.

A 3-db coupler, then, corresponds to  $p(u) = \frac{-1}{\sqrt{2\pi}} \frac{\sin^2 u/2}{u/2}$ . A perfectly

flat coupling level would require inclusion of all side lobes of  $p(u)$  from  $u = -\infty$  to  $+\infty$  and hence would be infinitely long. By truncating  $p(u)$  at some point in  $u$ , an approximation to the desired coupling can be obtained. The general classification of couplers having periodic zeros in  $p(u)$  is based on the truncation of equation (9) which exhibits periodic zeros in the sine function.

The Fourier integral computer was used to investigate the approximation problem. A polar recorder was used on the output to permit plotting several solutions on one sheet for purposes of comparison. A series of five runs was made. The first run used the first positive and first

negative lobe of  $\frac{\sin^2 u/2}{u/2}$  as an input. Positive and negative lobes must

be paired together to preserve the symmetric nature of the design. The next run consisted of the first two positive and first two negative lobes of the same function; more lobes were included, a pair at a time, in subsequent runs. The results are plotted in Figure 5. As is evident from the figure, the addition of a side lobe pair increases the number of ripples in the output response by one unit. Also evident from the set of responses is the fact that Gibbs' overshoot is present and does not decrease in amplitude with increasing coupler order (number of side lobes used).

Ripple level may be equalized by using weighting techniques often employed in antenna array synthesis. The ordinates of symmetrically disposed side lobes can be weighted with Dolph-Chebyshev coefficients to produce approximate equal-ripple performance. Better results can be obtained by appropriate use of a weighting function derived from the equal-ripple trigonometric polynomials used in the synthesis of stepped-coupler designs. As an example, consider the following digitally generated ninth-order polynomial which approximates the constant, unity, in an exact equal-ripple manner ( $\pm 5$  percent voltage) over the interval  $0 < \theta < \pi$ :

$$f(\theta) = 1.2626 \sin \theta + 0.3931 \sin 3\theta + 0.2049 \sin 5\theta + 0.1170 \sin 7\theta + 0.0927 \sin 9\theta \quad (10)$$

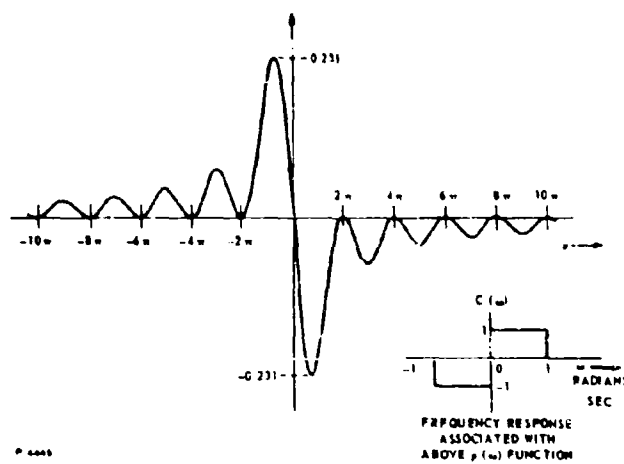


Figure 4 - Plot of  $P(u) = -\frac{1}{\pi} \frac{\sin^2 u/2}{u/2}$

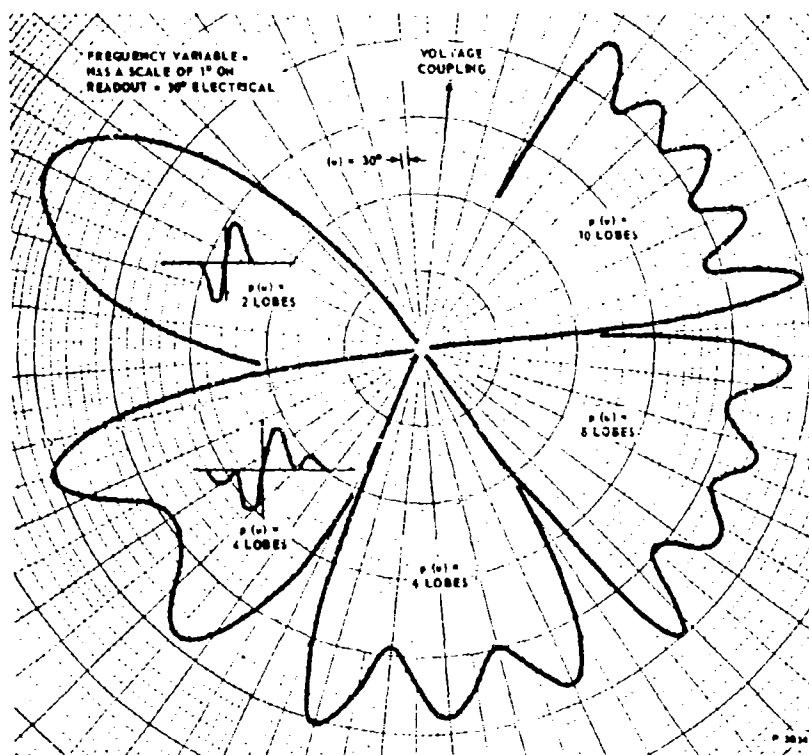


Figure 5 - Frequency Response of Various Truncations of  $p(u) = \frac{\sin^2 u/2}{u/2}$

The conventional Fourier representation in the same interval is given by

$$g(\theta) = \frac{4}{\pi} \left( \sin \theta + \frac{1}{3} \sin 3\theta + \frac{1}{5} \sin 5\theta + \frac{1}{7} \sin 7\theta + \frac{1}{9} \sin 9\theta \right). \quad (11)$$

Numerical evaluation of  $g(\theta)$  will exhibit the usual Gibbs' overshoot phenomenon. The desired weighting function is obtained from that set of coefficients which, when multiplied by the Fourier coefficients in  $g(\theta)$ , gives the coefficients of the true equal-ripple function  $f(\theta)$ . Thus

$$\begin{aligned} w_1 &= 1.2626/(4/\pi) = 0.992 \\ w_3 &= 0.3931/(4/3\pi) = 0.929 \\ w_5 &= 0.2049/(4/5\pi) = 0.805 \\ w_7 &= 0.1170/(4/7\pi) = 0.643 \\ w_9 &= 0.0927/(4/9\pi) = 0.656 \end{aligned} \quad (12)$$

The above weighting coefficients, derived from a discrete Fourier series representation of constant coupling, can be applied to the distributed coupling case in the following manner:

The first weighting coefficient,  $w_1$ , multiplies the ordinates of the first positive and negative lobes of  $-\frac{1}{\pi} \frac{\sin^2 u/2}{u/2}$ , which extend to

$|u| = 2\pi$ , as can be seen in Figure 4. The next coefficient,  $w_3$ , multiplies the ordinates of the second set of lobes for  $|u|$  values between  $2\pi$  and  $4\pi$ , etc. All five weighting coefficients given in equation (12) were applied in this manner to the  $p(u)$  function of equation (9). The Fourier integral computer was then used to obtain the coupling response of the weighted function,  $p_w(u)$ .

The resultant coupling is very close to true equal ripple. Because of computer noise, the exact amount of ripple is difficult to determine precisely, but it is approximately  $\pm 4$  percent in voltage. This may be compared with the  $\pm 5$  percent voltage ripple associated with the original equal-ripple polynomial from which the weighting function was derived. A more careful analysis using a digital computer to obtain more precision would be desirable. The foregoing weighted function,  $p_w(u)$ , may with proper normalization be used directly to synthesize various approximate equal-ripple, loose-coupling (first-order) designs.

Couplers designed with the aid of first-order theory, employing weighting coefficients such as given in equation (12), will not exhibit flat coupling for multi-octave bandwidth designs of mean-coupling level greater than approximately -10 db. A higher order theory is required to describe adequately the effects involved. Fortunately, a closed-form technique, described below, has been found which permits weighting the  $p(u)$  function in a manner that both eliminates Gibbs' overshoot and



includes the compensation for tight coupling as required by higher-order theory. This technique uses weighting functions derived from exact stepped-coupler designs [1]. Figure 6 depicts a weighted fifth-order  $p_w(u)$  function and the associated coupling with distance ( $k$  versus  $u$ ) and coupled frequency response ( $|C|$  versus  $\omega$ ).

A description of stepped couplers, in terms of the  $p(u) = \frac{1}{2} \frac{d}{du} \ln Z_{oe}(u)$  domain, is required in the process of obtaining the desired weighting function. The coupling coefficients of stepped couplers change discontinuously, so that  $p(u)$  consists of a set of Dirac delta functions located periodically with distance at the discontinuities. The area under each delta function is given by  $\frac{1}{2} \ln \left( Z_{i+1}/Z_i \right)$ , where  $Z_i$  and  $Z_{i+1}$  are the even-mode impedances on either side of the discontinuity. Under these conditions, one can show by using equation (4) that

$$C(\omega) = j e^{-j \frac{\omega d}{v}} \sum_{n=1}^{\frac{N+1}{2}} \ln \frac{Z_{\frac{N+3}{2} - n}}{Z_{\frac{N+1}{2} - n}} \sin (2n - 1) \frac{\omega d}{Nv} \quad (13)$$

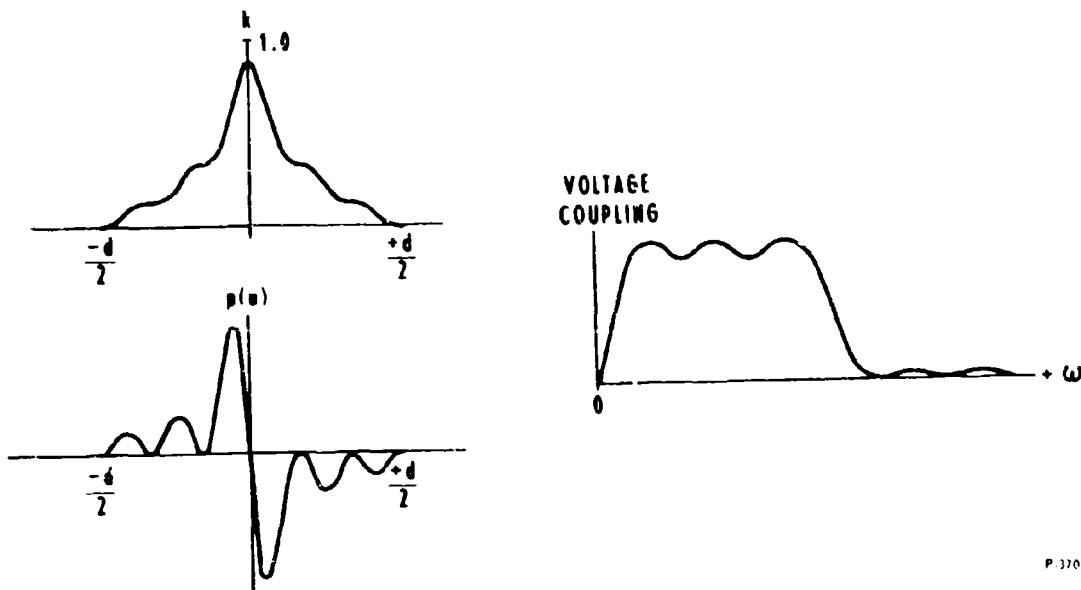


Figure 6 - Response of a Typical Periodic  $p(u)$  Coupler

where  $N$  is the order of design. (The equal-ripple polynomial listed previously, equation (10), is of order  $N = 9$ , with  $\theta = \frac{\omega d}{Nv}$ .) In this notation,  $Z_0$  is the impedance of the connecting lines (one ohm),  $Z_1$  is the impedance of the outermost coupled line in the structure,  $Z_2$  is the impedance of the next adjacent section, etc. The impedance of the center section is  $\frac{Z_{N+1}}{2}$ .

The Fourier series representation of unity voltage level covering the same band as the above stepped design is given by

$$|C(\theta)| = \frac{4}{\pi} \sum_{n=1}^{\frac{N+1}{2}} \frac{1}{2n-1} \sin(2n-1)\theta. \quad (14)$$

Equation (14) exhibits Gibbs' overshoot and further is valid only for small coupling (first-order) as an expression describing the response of a coupler. Equation (13) contains a correction for both Gibbs' overshoot and higher-order coupling effects. The desired weighting function consists of the terms of equation (13) divided by those of equation (14):

$$W_n = \frac{\pi}{4} (2n-1) \frac{\ln\left(\frac{Z_{N+1}}{2} - n\right)}{\ln\left(\frac{Z_{N+1}}{2} - n\right)} \quad (15)$$

where:  $1 \leq n \leq \frac{N+1}{2}$  in integer steps.

The weighting terms given for the discrete jump case by equation (15) can be applied directly to equation (9), which is the tapered-coupling Fourier representation of unity voltage level.  $W_1$  multiplies the two central lobes of  $p(u)$  from  $-2\pi$  to  $+2\pi$ ,  $W_2$  multiplies the next two lobes of  $p(u)$  from  $-4\pi$  to  $-2\pi$  and from  $+2\pi$  to  $+4\pi$ , etc., to produce the weighted function  $p_w(u)$ . The resulting tapered design should provide essentially the same bandwidth, ripple tolerance, and mean coupling level as the stepped prototype used to obtain the weighting function.

The even-mode characteristic impedance of the distributed coupler can be obtained by processing the weighted distribution,  $p_w(u)$ . An  $N^{\text{th}}$  order coupler is  $(N+1)2\pi$  units long in  $u$ , running from  $-(N+1)\pi$  to  $+(N+1)\pi$ . Coupling is zero at  $u = -(N+1)\pi$ , so that  $Z_{oe}(u) = 1$  at that point. Equation (5) can thus be rewritten:

$$Z_{oe}(u) = \exp \left[ 2 \int_{u=-(N+1)\pi}^u p_w(u) du \right] \quad (16)$$

The integral indicated in equation (16) is given by the integral of equation (9), since  $p_w(u)$  consists of equation (9) weighted over various  $2\pi$  intervals by constants (given by equation (15)). Fortunately, the integration can be found in tabular form by noting that

$$2 \int_0^a \frac{\sin^2 u/2}{u} du = \int_0^a \frac{(1 - \cos u)}{u} du = \text{Cin}(a) \quad (17)$$

where Cin is one definition of the cosine integral. The Cin is tabulated in King [5] for arguments through 25. Alternately, one might note that  $\text{Cin}(a) = C + \ln a - \text{Ci}(a)$ , where  $C = 0.5772$ , is Euler's constant, and that  $\text{Ci}(a)$  is an alternate form of cosine integral tabulated in a number of references [6,7]. The integrand function,  $2 \frac{\sin^2 u/2}{u}$ , has minima every  $2\pi n$  radians and has maxima where  $\tan u = 2u$ . Solutions to the latter equation are tabulated in Reference [8]. For high-order side lobes, the maxima tend to fall halfway between the minima.

The actual physical length of the coupled region,  $d$ , can be determined once the desired center frequency,  $f_c$ , of the equal-ripple band has been chosen. This length is given by

$$d = \frac{(N+1)2\pi}{2\pi} \frac{\lambda_c}{4} = \frac{(N+1)v}{4f_c} \quad (18)$$

$Z_{oe}(u)$  can be rescaled in terms of the actual physical dimensions by noting that  $d$  corresponds to  $(N+1)2\pi$  units in  $u$  in the prototype design. It is interesting to note that equation (18) states that the equal-ripple tapered-line coupler is exactly one-quarter wavelength longer than the equivalent stepped-impedance coupler.

Figure 7 compares the coupling coefficient for ninth-order 8.34 db, tapered-line design with that of the stepped coupler from which the weighting coefficients were derived. It is evident that the stepped coupler and the tapered-line coupler are related. The tapered-line coupler is about 11 percent longer than the stepped design and requires  $k_{\max} = 0.727$  in comparison with  $k_{\max} = 0.672$  for the stepped design. This result is characteristic of the difference between tapered and stepped designs.

The rate of change of coupling with distance is more gradual in the tapered-line design, as is apparent from Figure 7. Approximately one-quarter wavelength is utilized in tapering between coupling plateaus in the periodic-zero tapered line model. The abrupt changes in coupling in the corresponding stepped model occur at the center of the tapered regions at the points of maximum rate of change of coupling versus distance. As mentioned in the Introduction, practical stepped couplers cannot exhibit perfectly abrupt changes in coupling. The present theory shows that rather

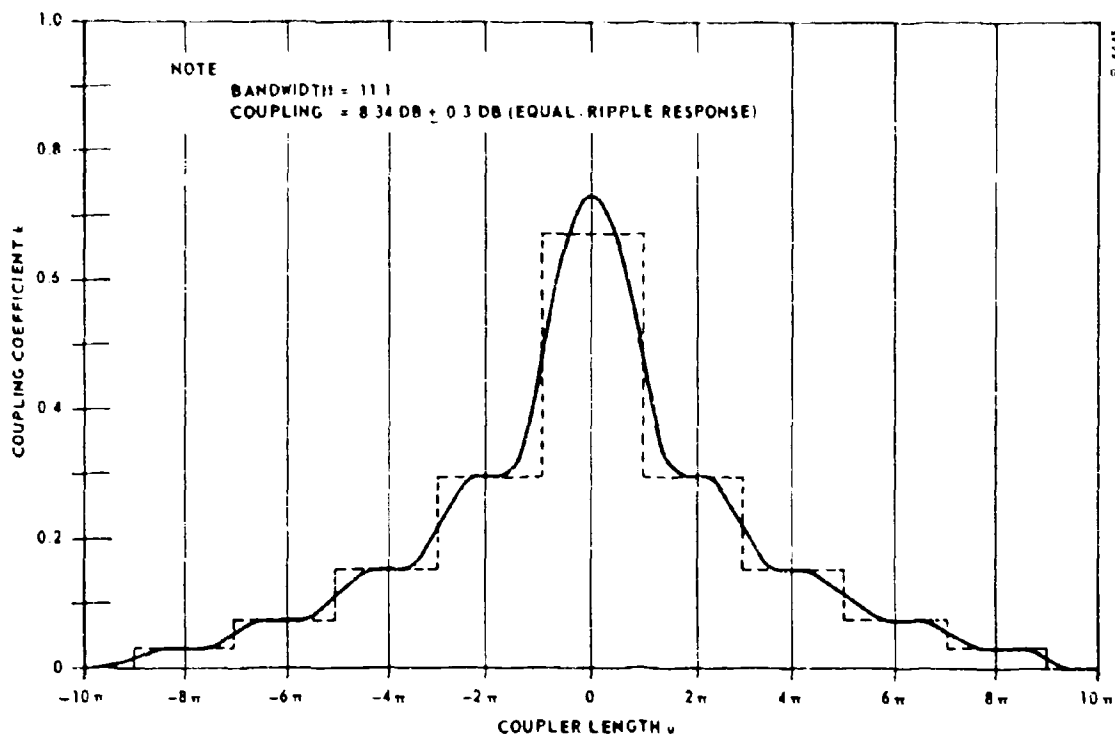


Figure 7 - Physical Coupling Versus Distance for a Tapered-Line Coupler and a Stepped-Coupler which Provide Essentially Identical Coupling Versus Frequency Performance

gradual transitions can, in fact, be used while preserving essentially similar response. The chief difference relates to repetitious coupling response at frequencies above the first coupling band: the mathematical model for the ideal stepped coupler repeats at center frequencies which are odd harmonics of the fundamental out to infinite frequency, whereas the periodic-zero tapered line coupler exhibits essentially zero coupling beyond the first pass band. Practical stepped couplers will exhibit fairly good third harmonic response and possibly higher coupling bands will be present in lower frequency designs where the transition regions are a small fraction of a quarter wavelength. For higher frequency models, repetition of the second coupling band is typically of poor shape and mean-coupling is lower than the design level showing the presence of appreciable tapering in the physical model.

## 2.4 SYNTHESIS OF THE 800-11,000 MHz COUPLER

The 800-11,000 MHz band can be covered by a tandem interconnection of two identical 8.34 db couplers of ninth-order design. However, the overall ripple tolerance is rather close to the 1 db maximum coupling unbalance allowed in the specification. An eleventh-order ( $N = 11$ ) design was used which exhibited a more acceptable ripple tolerance. It was, however, necessary to synthesize a set of eleventh-order stepped coupler impedances to provide the weighting functions used in the design of the tapered-line coupler, since the tables of Reference [1] cover only through the ninth-order designs.

Synthesis of the stepped designs was accomplished on a Control Data G-20 computer. Direct synthesis by application of Richard's theorem, as outlined in [1], becomes difficult for designs of eleventh-order due to the sensitivity of successive steps to roundoff error of preceding steps. It was not possible to employ double precision arithmetic in the computer due to the limitations of the subroutine decks available, so that an alternate synthesis procedure had to be employed. Equal-ripple trigonometric polynomials which provide an exact description of the desired coupling response [1] were generated by an iterative technique. These functions were then used in an iterative synthesis procedure.

A coupler design having approximate equal-ripple response can be obtained by setting equation (13) equal to the desired response in terms of the equal-ripple trigonometric polynomial. The coupler so designed is then analyzed exactly (by using ABCD cascade matrices), and an error curve is formed by taking the difference between the actual response and the desired response. A Fourier analysis of the error curve gives correction terms to be added to the approximate coupler design. A new analysis is made permitting higher corrections to be made. Iterations made as outlined converge to the desired solution. The iterative technique employed is similar to that described by Shelton [9] except that exact equal-ripple functions have been employed, along with a different expression for first-order coupler response in terms of the parameters of the coupler (equation (13)).

The final design chosen theoretically exhibits  $8.34 \pm 0.33$  db coupling over a 14.07:1 bandwidth; this results in a  $3.01 \pm 0.27$  db coupling for a tandem interconnection of two units. The 800-11,000 MHz specification is equivalent to a 13.75:1 bandwidth, so that some margin has been provided both in bandwidth and in coupling ripple. The computer generated even-mode impedance data for the applicable stepped coupler is given below using the other terminology of equation (13):

$$\begin{aligned}
Z_1 &= 1.031 \\
Z_2 &= 1.064 \\
Z_3 &= 1.121 \\
Z_4 &= 1.221 \\
Z_5 &= 1.430 \\
Z_6 &= \frac{Z_{N+1}}{2} = 2.376
\end{aligned}
\tag{19}$$

This data may be used to calculate the required weighting functions described by equation (15). Thus

$$\begin{aligned}
W_1 &= \frac{\pi}{4} (2 \cdot 1 - 1) \ln \frac{Z_6}{Z_5} = 0.399 \\
W_2 &= \frac{\pi}{4} (2 \cdot 2 - 1) \ln \frac{1.430}{1.221} = 0.372 \\
W_3 &= \frac{\pi}{4} (2 \cdot 3 - 1) \ln \frac{1.221}{1.121} = 0.336 \\
W_4 &= \frac{\pi}{4} (2 \cdot 4 - 1) \ln \frac{1.121}{1.064} = 0.287 \\
W_5 &= \frac{\pi}{4} (2 \cdot 5 - 1) \ln \frac{1.064}{1.031} = 0.229 \\
W_6 &= \frac{\pi}{4} (2 \cdot 6 - 1) \ln \frac{1.031}{1} = 0.256
\end{aligned}
\tag{20}$$

The weighting terms given by equation (20) are applied to  $p(u)$  given by equation (9) over the proper  $2\pi$  intervals discussed previously ( $W_1$  multiplies  $p(u)$  from  $-2\pi \leq u \leq 2\pi$ , etc.). The  $p_w(u)$  so defined can then be substituted into equation (16) producing a curve of  $Z_{oe}(u)$ . This may in turn be substituted into equation (8) to obtain a curve of coupling versus distant,  $k(u)$ .

The actual length of the individual couplers can be determined by equation (18). It is intended that the coupler be built in irradiated polyolefin for which  $v = 77.5 \times 10^8$  inches/sec. The 14.07:1 bandwidth of the theoretical design was distributed so as to cover 800 to 11.256 MHz. The midpoint of the coupling band is accordingly

$$\frac{11.256 \times 10^9 + 0.800 \times 10^9}{2} = 6.028 \times 10^9 \text{ Hz.}$$

Equation (18) gives

$$d = \frac{(11 + 1) \cdot 77.5 \times 10^8}{4 \cdot 6.028 \times 10^9} = 3.86 \text{ inches} \quad (21)$$

One can renormalize the  $k(u)$  curve to fit the 3.86 inch length required by noting that 3.86 inches corresponds to  $(11 + 1)2\pi = 24\pi$  in  $u$ . The results of this procedure are shown plotted in Figure 8. The coupling coefficient required at the center of each 8.34 db coupler is 0.753. The stripline geometry employed to obtain this coupling level is discussed in Section 3.

## 2.5 SYNTHESIS OF A 390-11,000 MHz COUPLER

The 390-11,000 MHz band represents a 28.2:1 bandwidth ratio, which is slightly more than double the bandwidth of the preceding design. The maximum value of coupling coefficient required in a two-coupler tandem design cannot be practically achieved in three-layer stripline due to the extremely thin dielectric center shim required. Bandwidths of this magnitude can, however, be achieved by connecting three couplers in tandem. A mean coupling coefficient of 11.74 db is required from each to provide a mean 3.01 db overall coupling level.

Various 15<sup>th</sup>, 17<sup>th</sup>, 19<sup>th</sup>, and 21<sup>st</sup> order equal-ripple 11.74 db stepped couplers were synthesized using the iterative techniques outlined

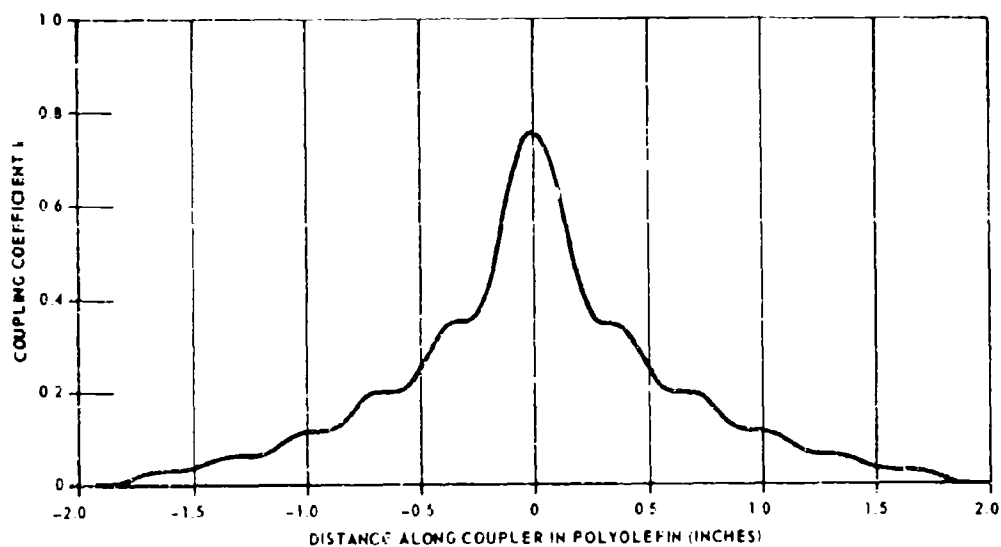


Figure 8 - Equal Ripple (800 MHz-11,256 MHz) Coupler

in the preceding section. From the standpoint of a realistic ripple tolerance, the 21<sup>st</sup> order couplers provide the most acceptable performance: a 28.56:1 bandwidth can be achieved with an associated coupling value of approximately  $3.01 \pm 0.33$  db for three 11.74 db units in tandem. The coupler consists of the following even-mode impedances:

$$\begin{aligned} Z_1 &= 1.017 \\ Z_2 &= 1.027 \\ Z_3 &= 1.039 \\ Z_4 &= 1.055 \\ Z_5 &= 1.075 \\ Z_6 &= 1.102 \\ Z_7 &= 1.138 \\ Z_8 &= 1.190 \\ Z_9 &= 1.268 \\ Z_{10} &= 1.415 \\ Z_{11} &= 1.980 \end{aligned} \quad (22)$$

The foregoing impedances may be substituted into equation (15) to obtain weighting functions required in the design of the tapered-line coupler. The weighting functions are applied to equation (9) over the proper intervals to give  $p_w(u)$ , which can be substituted in equation (16), to give  $Z_{oe}(u)$ . The coupling versus distance characteristic,  $k(u)$ , then follows from equation (8).

The results of the foregoing procedure have not been calculated in detail, since the calculations are lengthy. It is, however, possible to present a simple design procedure which gives a close approximation to the desired results. It can be noted from Figure 7 that the tapered coupling coefficient is essentially equal to that of the corresponding stepped design at the center of the quarter-wave sections of the latter design. Coupling can also be compared at the step discontinuities, where the tapered design is about equal to the mean value of the jump present at the steps. If a  $(1 + \cos u/2)$  curve shape is used to taper between the points of zero slope the design will be close to that predicted by the exact method over a majority of the coupler length. The exact description should be used for the central portion of the design, e.g., from  $u = -4\pi$  to  $+4\pi$ , where this approximation departs from the previously described solution.



The center coupling required in the tapered-line design can be determined from the foregoing approximation. The value of  $Z_{oe}$  ( $u = -4\pi$ ) should closely correspond to that of the stepped design. According to Figure 7, that point falls in the middle of the third element of the stepped design, which, in the coupler of equation (22), is  $Z_9 = 1.268$  ohms. The approximation states mathematically that the area under the  $p(u)$  curve from the outer edge of the coupler at  $u = -(21 + 1)\pi$  to  $u = -4\pi$  should result in  $Z_{oe}(-4\pi) = 1.268$ , that is,

$$\int_{-22\pi}^{-4\pi} p_w(u) du = \frac{1}{2} \ln Z_{oe}(-4\pi) = 0.1186 .$$

The remaining portion of the integral from  $-4$  to  $0$  can be obtained from equations (9), (15), and (17):

$$\int_{-4\pi}^0 p_w(u) du = \frac{1}{\pi} \left[ W_2 (\text{Cin } 4\pi - \text{Cin } 2\pi) + W_1 (\text{Cin } 2\pi - \text{Cin } 0) \right]$$

where

$$W_1 = \frac{\pi}{4} (2 \cdot 1 - 1) \ln \frac{1.980}{1.415} = 0.2640$$

$$W_2 = \frac{\pi}{4} (2 \cdot 2 - 1) \ln \frac{1.415}{1.268} = 0.2585$$

Accordingly,

$$\int_{-4\pi}^0 p_w(u) du = \frac{1}{\pi} \left[ 0.2585 (3.114 - 2.438) + 0.2640 (2.438 - 0) \right] = 0.2604$$

and

$$\frac{1}{2} \ln Z_{oe}(0) = \int_{-22\pi}^{-4\pi} p_w(u) du + \int_{-4\pi}^0 p_w(u) du = 0.1186 + 0.2604 = 0.379 .$$

The even-mode impedance at the coupler center,  $\exp(2 \times 0.379)$ , is equal to 2.135 ohms, which may be compared with the 1.98-ohm level present in the stepped design. The impedance as calculated should be very close to the more exact value which would be calculated from the in function with appropriate weighting terms evaluated over the entire coupler length. A 2.135-ohm impedance corresponds to  $k = 0.640$ , as determined from equation (8). This value of coupling is well within the range which can be easily realized in three-layer stripline [10].

The length of the coupler can be determined from equation (16). The mid-frequency of the coupler is

$$f_c = \frac{0.390 \times 10^9 + 11,000 \times 10^9}{2} = 5.69 \times 10^9 \text{ Hz}$$

If polyolefin line is employed,  $v = 77.5 \times 10^8$  in/sec and

$$d = \frac{(21 + 1) \times 77.5 \times 10^8}{4 \times 5.69 \times 10^9} = 7.48 \text{ inches.}$$

This coupler is almost twice as long as the 800-11,000 MHz design.

One of the chief difficulties constructing extremely broadband couplers is the presence of insertion loss at the high frequency end of the band. A coupler which covers very low frequencies must inherently be long, so that the insertion loss of the structure becomes appreciable at the high end of the band, due to the normal increase in dielectric and copper losses with frequency. In addition, a larger number of units are connected in tandem in broadband designs to provide the extra mean coupling bandwidth product required, thereby directly adding extra length and loss to the structure.

One can determine approximately the insertion loss of the 390-11,000 MHz design from measurements made on the 800-11,000 MHz coupler and from loss measurements of a test section of polyolefin line. It is estimated that the overall line length from the input port to the transmitted port would be 24.75 inches. The insertion loss per unit length for the line geometry to be employed (0.062-inch thick ground plane boards with a small center shim) was measured to be about 0.055 db/inch at 11 GHz. A minimum of  $0.055 \times 24.75 = 1.36$  db insertion loss will thus be present in the coupler. Measurements on the 800-11,000 MHz coupler indicated that the excess loss due to the reduced linewidth in the middle of the coupler is too small to be differentiated from the basic loss calculation based on a uniform linewidth basis (less than 0.1 db difference). It is therefore predicted that the 390-11,000 MHz design would exhibit about 1.4 db insertion loss, maximum, at the high frequency end of the band.

For circuits that must withstand the rigors of temperature, polyolefin is not practical. The high-temperature resistant boards that must be employed, such as teflon-glass, exhibit considerably higher loss per unit

length than polyolefin, with a corresponding rise in coupler loss. Teflon-glass board, for example, would probably exhibit 3-db insertion loss at 11 GHz if used in the 390-11,000 MHz coupler.

### SECTION 3

#### CONSTRUCTION OF THE 800-11,000 MHz COUPLER

##### 3.1 DETERMINATION OF STRIPLINE COUPLING PARAMETERS

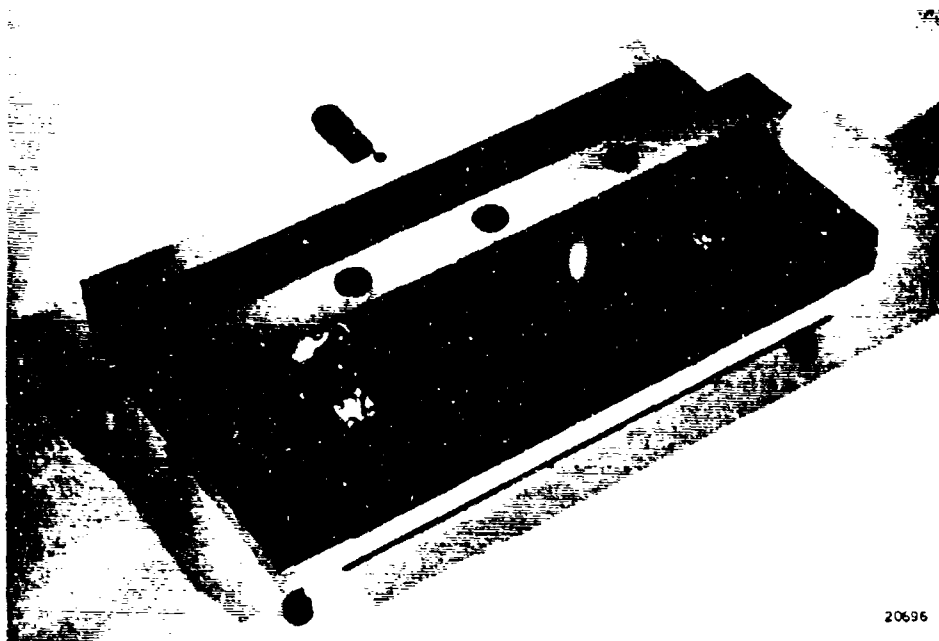
The coupler design described in Section 2.4 requires a coupling coefficient,  $k = 0.753$ , at the center. To assure maximum directivity, it is important that the design use fully overlapped coupling in the center to permit crossing of the conductors for purposes of tandem interconnection. A jog in the center caused by overly tight coupling of the lines would defeat the purpose of the tapered-line geometry.

To assure uniform ripple and high isolation, very accurate data on three-layer stripline coupling parameters is necessary. The data employed in the past was obtained from zero conductor thickness asymptotic solutions, such as found in Reference [10]. A 0.010-inch centerboard dielectric thickness, which might typically be used, is thin enough in comparison with 1-ounce copper foil (0.0014-inch thick) so as to cause noticeable deviation from the zero thickness approximation.

It is difficult to obtain useful conformal transformation solutions to the problem of finite conductor-offset stripline. Therefore, it was decided that a measurement program would be required to obtain data of the accuracy required. A three-layer stripline test fixture, Figure 9, was available to facilitate such measurements. A six-inch length of uniformly coupled line can be measured in the fixture. A broadband time domain reflectometer is used to ascertain that overlap has been properly adjusted for a given conductor width to assure that  $\sqrt{Z_{oe}Z_{oo}} = 50$  ohms. Coupling is then measured under matched conditions at the first quarter-wave frequency, which occurs in the vicinity of 300 MHz. The value of coupling measured is corrected for insertion loss effects which are fairly small at these frequencies.

The effect of foil thickness is of major concern only for tight coupling, where the two stripline members are overlapped. For loose coupled conditions, the zero thickness solution given by Shelton [10] may be applied with little error.

The directivity of a previously constructed 9th order design using 0.010-inch dielectric center shim was affected significantly by the physical pressure applied to the polyolefin stripline sandwich. The effect was virtually eliminated by using 0.001-inch teflon shim carefully placed next to the foil conductors of the coupler. This material largely fills the air space that is present, although careful cutting is required to permit a butt joint against the tapered geometry of the foil.



20696

Figure 9 -- Stripline Parameter Test Fixture

It was determined that polyolefin will exhibit continued cold flow under excessive pressure; the foil conductors depress into the center shim material. Addition of the teflon largely prevents this cold flow process by distributing the force applied to the sandwich. The difference the 0.001-inch teflon thickness and the 0.0014-inch foil thickness appears to have been largely eliminated by rubber cement employed to keep the teflon in place. Polyolefin is used in the 800-11,000 MHz design primarily because of its exceptionally low loss characteristics.

Measurements in the stripline test fixture were made with 0.001-inch teflon present next to the foil conductors. It would, of course, be preferable to use polyolefin shim, which is commercially available only in 0.002-inch minimum thickness. Little effect has been observed from the use of the 0.001-inch teflon due to the small amount involved and the relative similarity between the two dielectric constants (2.32 for polyolefin and 2.08 for teflon). It was found from a series of measurements that 0.008-inch polyolefin center board would give the desired 0.753 coupling for a fully-overlapped line geometry.

Stripline data was generated for 0.008-inch centerboard conditions. Each ground plane board is nominally 0.062-inch thick polyolefin, including the 1-ounce foil outer coating. Inherent in the geometry is the addition of the 1-mil shim material next to the foil conductors. Figure 10 shows the data generated. Data for tight coupling was measured in the test fixture, while loose coupling data ( $k < 0.4$ ) was obtained from Shelton's transformal solution for loose coupling [10]. The average thickness of the overall dielectric sandwich is about 0.130 inch, so that the normalized centerboard thickness which appears in Shelton's solution is given by  $s = 0.008/0.130 = 0.06154$ .

### 3.2 LAYOUT OF THE COUPLER

The desired coupling characteristic given in Figure 8 was translated into physical dimensions with the aid of Figure 10. According to Figure 8, zero coupling is desired at each end of the coupler, which would require an infinite separation between the coupled lines if it were to be realized.

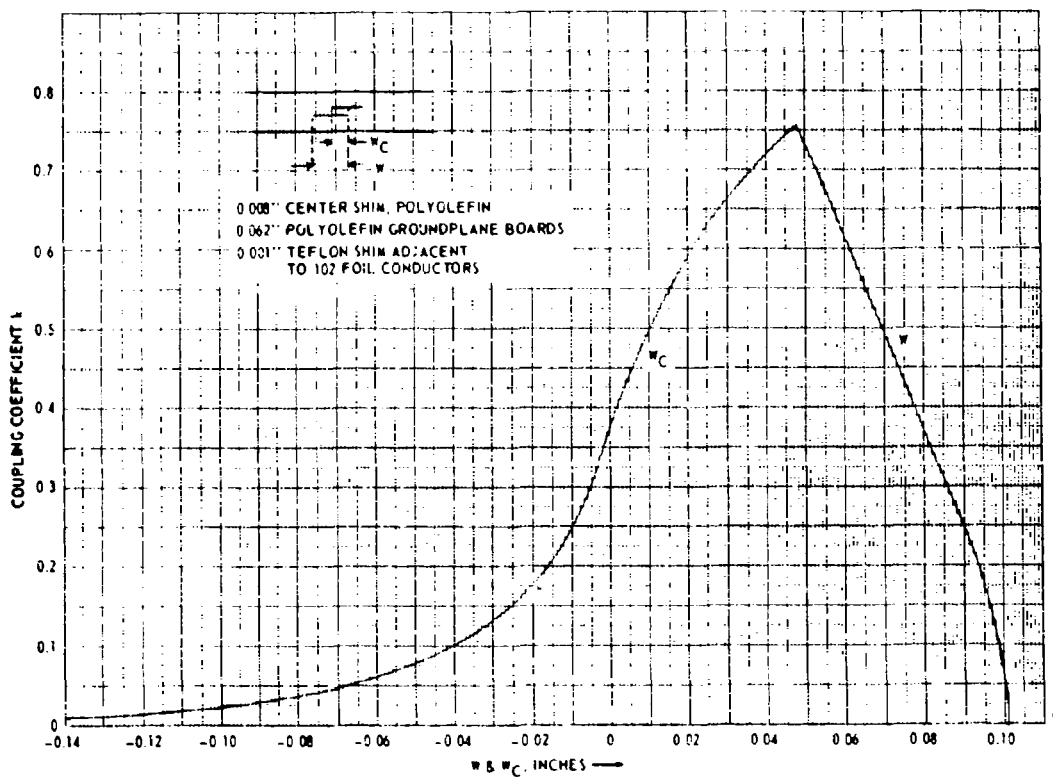
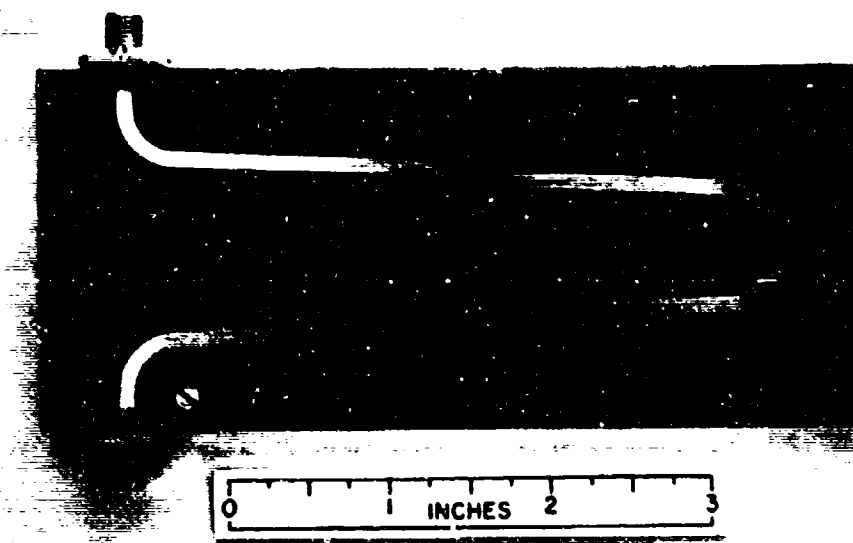


Figure 10 - Three-Layer Stripline Coupling Parameters

A drawing of the physical dimension predicted by Figures 8 and 10 was made. It exhibits a rapid change in spacing in the region between the last low coupling level plateau and the exterior of the design. A simple circular bend of interior radius 0.2524 inch was found to fit the layout over much of this region. The bend is continued for a full 90 degrees, so that where zero coupling is desired, the line is perpendicular to the axis of the coupler. Figure 11 shows the final layout of the coupler. The angle between the coupled lines in the circular arc region changes rapidly, which raises some question as to the exact nature of coupling achieved in the region. Measurements of the coupler made at low frequencies, for which this region is important, shows, however, very good correspondence to the theoretical design.

A 10X size artmaster of the entire coupler was cut on a G. Coradi Coradograph. Compensation was included for an expected 0.0007-inch over-etch per edge. A Roberston-Micro/Miltronix Minitor II plate camera was used to photo-reduce the design to full size. Carefully laid-out target centers were included to permit accurate dowelling of the two ground plane boards.

Electrical tests of models made from the foregoing negative indicated that the two-coupled sections are not identical due to unavoidable



23189

Figure 11 - Stripline Board

differences in cutting the artmaster. One side of the design exhibited consistently better isolation than the other by about 1 or 2 db. A second negative was made which used the better half of the artmaster with suitable masking and exposure to produce both coupled lines. This latter negative produced couplers of improved symmetry and higher mean isolation, including the final design.

### 3.3 CONSTRUCTION DETAILS

Simple 2.2" x 5" rectangular ground planes consisting of 3/16-inch thick aluminum plates are used in the final configuration. The ground plane and dielectric board sandwich is fastened with 18 socket head cap screws of 4-40 size, the heads of which are recessed into counterbores on one face of the coupler. The location of these screws is evident in Figure 11, consisting of three rows of holes, each row containing six holes. No special attempt has been made to connect the outer edges of the ground planes together since virtually no parallel plate mode has been detected in couplers of this type.

The most critical assembly operation concerns placement of the dowel holes through the polyolefin board target centers; the alignment of the stripline conductors depends entirely on the accuracy of this operation. The target centers on the polyolefin are carefully pricked with a sharp pin and drilled with successively larger drills until an 0.036-inch diameter hole for a dowel pin is produced. Standard steel paper clips are used for dowels.

Dowel holes are drilled through the aluminum ground planes in spots located from the holes previously fabricated in the polyolefin stripline boards. Care is taken to assure that these holes fall on the centerline of the case, although exact placement is not critical. The polyolefin boards are then each secured to the aluminum ground planes with countersunk No. 2 flat head screws, the location of which is shown in Figure 11. The screws remove most of the tendency for the polyolefin board to curl up.

The basic connector employed on the coupler is of the BRM-OSM variety. The earlier models employed Bendix (Dage) 31042-1 panel mounting female connectors with the back cable connection machined away. The connector is flush mounted to the edge of the ground plane stripline sandwich, as is evident in Figure 12. The centerpin of the connector is designed to accept 0.036-inch diameter stock, corresponding to the center conductor of 0.141-inch coaxitube. A suitably tapered pin made of stock of this size is used to connect to the stripline. Cerro Bend low melting point solder is used to attach the tapered pin to the stripline. The center polyolefin shim is cut away to accommodate the tapered connector pins in the overall sandwich.

Later models of the coupler were constructed using Omni-Spectra 204 flange mount female OSM connectors. The body of this particular design is intended for flush mounting and hence does not have to be machined.



The same taper pin is employed, the pin being soldered into a hole drilled into the solid center pin of the OSM connector. The OSM design does not use a retainer ring to hold the teflon insulation of the connector in place, but rather relies on a force fit of the teflon insulator into the connector shell for retention. This latter feature has been found to be of great value in reducing connector VSWR in the X-band region. An improvement of several db in isolation across X band resulted from incorporation of the OSM design. The overall VSWR of the mated connector and the associated transition into stripline has been difficult to determine because of the low value involved, but is well below 1.1:1 through X band. The basic BKM-OSM style connectors were chosen for the coupler because of the low VSWR that could be achieved in the transition to stripline.

The final coupler is shown in Figure 12. The apparent isolation of a 90-degree hybrid depends directly on the VSWR of the loads used to terminate the unused ports. A set of two low VSWR loads was constructed

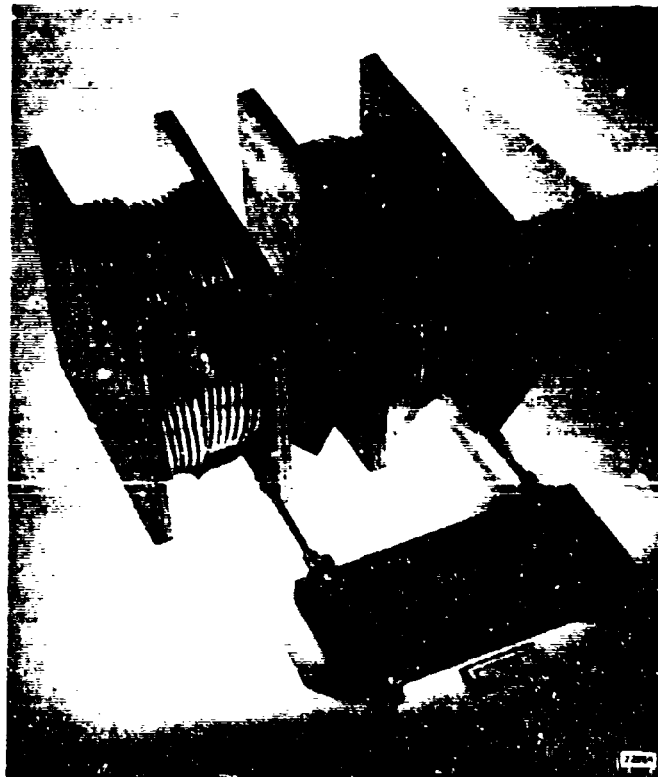


Figure 12 - 800-11,000 Mhz Coupler with Precision Test Loads

for use in the isolation measurement. These loads, also shown in Figure 12, each consist of a standard 50-ohm miniature load padded with 20 feet of precision coaxial cable. The insertion loss of the cable, which rises with frequency, pads out the VSWR of the miniature loads which tends also to increase at the higher frequencies. The small residual VSWR of the loads is readily identified on an isolation plot, since it exhibits extremely rapid variation with frequency due to the long line length present between the actual load and the coupler. The loads were delivered with the coupler as an end item, permitting verification of the data presented in this report. It is unimportant as to which load is used on which port of the coupler, due to the low residual VSWR involved.

## SECTION 4

### OPTIMIZATION OF THE 800-11,000 MHz DESIGN

#### 4.1 MODIFICATION OF THE CENTER SHIM

The first experimental model constructed showed an overcoupling throughout the frequency band. Fourier analysis indicated that the problem was due to overcoupling in the central region of the individual 8.34 db couplers. It has not been possible to ascertain the specific source of the difficulty. A much improved coupling characteristic was obtained by changing from 8-mil polyolefin centerboard to 9-mil centerboard, along with removal of the 1-mil teflon adjacent to the 1-ounce copper foil conductors. The conductors deform the 9-mil polyolefin shim slightly but careful tightening of the stripline sandwich prevents continued cold flow.

Changing the centerboard thickness has virtually no effect on coupling over the majority of the coupler length (see Reference 10). Only the central region of the design where the lines are nearly fully overlapped is affected, permitting selective adjustment of physical coupling present in that region. The measured isolation of the coupler design was improved by the use of 9-mil material.

Measured coupling matches the design theory of Section 2 rather well for all frequencies to about 10 GHz. Beyond that frequency, a droop in coupling occurs which results in greater than 1 db output unbalance in the vicinity of 10.5 GHz. The precise cause of the effect is not clear. The problem again is thought to be contributed to by the center region of the individual 8.34 db couplers. The coupling values change significantly in this region, as is evident in Figure 8. The assumption is made that coupling data of Figure 10 can be used throughout the central region without modification. However, the lines so designed vary rapidly so that a moderate angle exists between the lines for some distance. The actual rate of change of coupling achieved thus deviates to some extent from that desired.

A simple modification was found which brings the performance of the coupler within specification. The rate of change of coupling with distance is modified by the addition of a thin, specially cut dielectric shim to the center of both 8.34 db couplers. The shim consists of 1-mil teflon, 0.47 inch in width covering the coupled region associated with the two central lobes of the  $p(u)$  function. A square hole 0.1 by 0.1 inch is cut in the shim at the center of each coupled section where the lines overlap. The rapid increase and decrease in coupling that occurs at the edges of the hole gives rise to a high-frequency coupling component which compensates for the droop of the unmodified design. Although the rapid 1-mil change in dimension represents, in effect, a step change in

coupling, the step is relatively small and the geometry involved does not harbor large fringing capacities. Isolation is virtually unaffected by the presence of the shim. In assembling the overall sandwich, the central region is of necessity deformed by the foil conductors. Careful tightening of the screws fastening the case prevents continued cold flow of the polyolefin shim after the initial deformation.

#### 4.2 SUGGESTED DESIGN IMPROVEMENT

Although satisfactory and reproducible results were obtained by the use of a nonuniform shim, it would have been desirable to eliminate the shim for constructional convenience. Compensation for droop at the high-frequency end of the band can be constructed into the device by deliberate predistortion of the response characteristic. Instead of using a  $p(u)$  function for constant coupling as given by equation (9), one can derive a new  $p(u)$  function for the case of constant coupling with a high-frequency compensation ramp, as shown in Figure 13. The proper choice of break point in frequency,  $a$ , and the amount of predistortion required,  $\Delta$ , can be determined from measurement on the unmodified coupler. The new  $p(u)$  function corresponding to Figure 13 can be shown to be

$$p_{\Delta}(u) = \frac{1}{\pi} \left[ \frac{1}{u}(1 + \Delta)\cos u - \frac{1}{u} + \frac{\Delta}{(1-a)u^2} (\sin au - \sin u) \right]$$

A plot of this function for negative values of  $u$  appears in Figure 14 for the choice of constants,  $a = 0.728$  and  $\Delta = 0.122$ . This choice corresponds approximately to a breakpoint of 8 GHz in a coupler with an 11 GHz cutoff; the amplitude at the 11 GHz point is 1 db above the level in the plateau below 8 GHz. It will be noted that  $p(u)$  exhibits negative values in the vicinity of  $-2\pi$ ,  $-4\pi$ ,  $-6\pi$ , etc., which results in small-amplitude periodic reversals in coupling, as indicated by Equation (16). The shape of the  $p_{\Delta}(u)$  curve is quite close to that of the unmodified  $p(u)$  function, since a small amount of predistortion is involved.

Coupler synthesis would employ the same weighting coefficients indicated by Equation (15) applied over the respective  $2\pi$  intervals, as indicated previously. The resulting coupler will exhibit extra coupling at the high-frequency end of the band without resorting to nonuniform shimming techniques. A judicious choice for the constants  $a$  and  $\Delta$  should permit meeting the desired coupling specification upon first trial.

#### 4.3 MEASURED COUPLER PERFORMANCE

Coupling and isolation of the final delivered model are shown in tabular form below 1 GHz in Table I. Swept plots of coupling, transmission, and isolation are presented for L, S, C and X bands in Figures 15 through 18 with port 1 used as an input\*. Since the symmetry

\* Figures 15 through 25 are on pages 36 through 40.

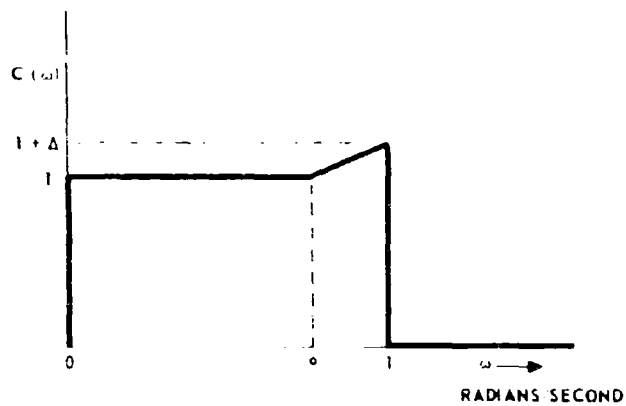


Figure 13 - Predistorted Coupler Response Characteristic

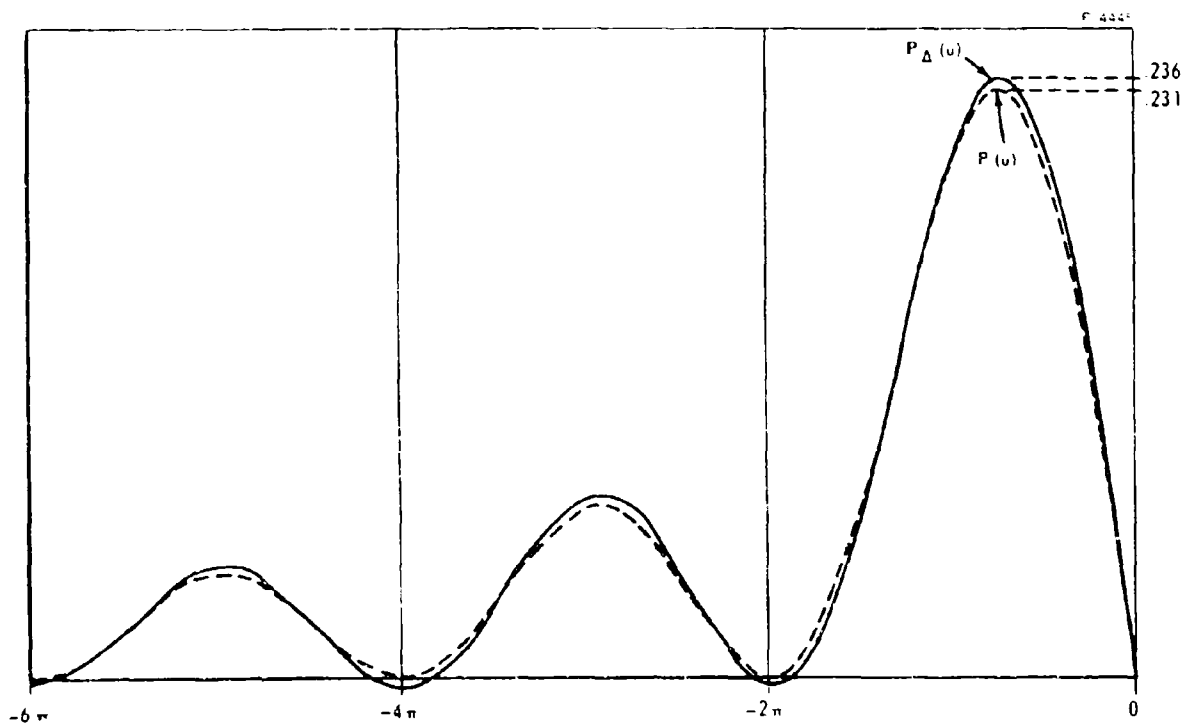


Figure 14 - Comparison Between the Flat  $P(u)$  and the Predistorted  $P_{\Delta}(u)$  Characteristics

Table 1 - UHF Performance of Coupler

Coupling:

f, MHz	Input: Port 1		Input: Port 3	
	C <sub>db</sub> (Port 3)	T <sub>db</sub> (Port 2)	C <sub>db</sub> (Port 1)	T <sub>db</sub> (Port 4)
750	3.68	2.68	3.75	2.75
800	3.37	2.83	3.38	2.82
850	3.20	2.98	3.20	2.98
900	3.08	3.08	3.08	3.08
950	3.12	3.27	3.12	3.27
1000	2.85	3.15	2.95	3.25

NOTE: Isolation: Greater than 30 db, either side, f < 1000 MHz

of the design is important, similar plots are presented in Figures 19 through 22 for an input to port 3, located on the other side of the coupler, as can be seen in Figure 12. Comparison of data taken with the different input ports indicates a high degree of symmetry.

The reference line shown in all isolation plots corresponds to the measured insertion loss of two NPM Narda pads whose nominal insertion loss is 23 db. The actual measured amount of attenuation presented by these pads at various frequencies is as follows:

DC	23.00 db
6 GHz	23.60 db
10 GHz	24.45 db
12.4 GHz	24.90 db

The crystal detectors employed in the swept isolation measurements operate in the square law region, permitting calculation of isolation with respect to the reference plot. A point half way between the reference plot and the baseline thus corresponds to 3-db greater isolation than the reference.

All swept plots of isolation show a fine grain variation due to the long-line loads employed. The isolation of the coupler itself corresponds to the mean value of the fine grain structure. Figures 15 through 22 indicate that isolation is poorest in L band, being equal to 23 db at about 1.75 GHz. Isolation improves with increasing frequency, and is above the 25 db specification through the useful coupling region in X band. This behavior is in contrast to that realized by stepped designs, which tend to exhibit low isolation at the high end of the band. A second physically identical model, built subsequent to the contractual delivery, exhibited nearly identical performance, with a minimum L-band isolation of 24 db.

Figures 15 through 22 also show that very close to true equal-ripple performance has been achieved over all frequency bands except for the

upper portion of the X-band characteristic, as discussed previously. Power meter measurements at the point of maximum unbalance visible on the X-band swept plot (10.4 GHz) have shown that unbalance at that point is just equal to the 1-db maximum allowed. The theoretical design utilizes a small enough ripple factor to provide some margin in bandwidth at both ends of the band; in practice, the coupler meets the 1-db specification from about 750 MHz to 11,300 MHz, which is slightly greater than a 15:1 bandwidth. Insertion loss, measured with a padded bolometer at 11.3 GHz, is about 0.55 db, well within the 1-db maximum loss specification.

Because of the limited time available for testing within the delivery schedule, phase and VSWR measurements, which require point-by-point evaluation, were not made in all bands on the coupler that was delivered. Coupling and isolation of the second model are nearly identical to those of the delivered model. VSWR measurements were made at 200 MHz intervals starting at 2 GHz (the longest wavelength measurable within a BRM slotted line). Results of the measurements are given in Figure 23.

The original specification states that maximum allowable VSWR is to be less than 1.3 db, which corresponds to a maximum VSWR of 1.161:1 in voltage ratio. Figure 23 indicates that the maximum VSWR measured was 1.16:1. The VSWR's in Figure 24 are composites of residual slotted line VSWR, OSM connector VSWR, the VSWR of the transitions into stripline, and, finally, the intrinsic VSWR of the coupled-line structure. The VSWR of the intrinsic coupled structure therefore is thought to be considerably smaller than the composite numbers measured, so as to permit the cascading of hybrids and constant phase shifters within a stripline deck for antenna array excitation, etc.

The parameter most difficult to evaluate is the phase shift between the two output signals, which by specification, should be  $90 \pm 3$  degrees. The coupler itself provides output amplitudes which are equal to within 1 db, so that a phase bridge consisting of a slotted line can be placed across the output terminals directly. Normally, such a phase bridge would employ two phase-and-amplitude matched pads, one on each side of the line to reduce the influence of cable, device, and slotted-line VSWR on the phase measurement. The electrical center of the bridge is determined by alternately opening the cables leading to the device. The  $90^\circ$  phase shift thus is indicated by the location of the  $180^\circ$  points (nulls) in the line as measured with respect to the electrical degrees from the line center, corresponding to  $90^\circ$  total difference in phase of the two output signals.

Miniature pads of the quality required for this task are not available at the present time. The coupler itself possesses lower VSWR over the entire band than any available commercial padding. Measurements were made accordingly without pads in the bridge circuit. This, however, feeds the output signals unattenuated back into the coupler, thereby making phase measurements fully susceptible to perturbations from the finite isolation of the coupler. A signal 25 db down (the typical isolation of the coupler) will perturb the output of the opposed port

by 3.2 degrees, a measurement inaccuracy greater than the allowable tolerance on phase shift. Overall deviations as large as 9 degrees were recorded in such measurements taken without the use of attenuative padding.

A second set of measurements was made using 10-foot runs of coaxitube for padding. Figure 24 shows the measurement setup employed. Each 10-foot length of coaxitube provides about 3-db insertion loss at 5 GHz, or about 0 db at 10 GHz. The VSWR of such cable is quite low, as required. The electrical center of the bridge (the two 10-foot cables and the slotted line) is determined at each measurement frequency to guard against non-tracking dispersion in the long cables. A longer set of lines would have been desirable, but could not be obtained conveniently within the time period allotted to measurements. The cables reduce measurement error to approximately one-half, although the maximum possible error can, under adverse circumstances, still exceed the 3-degree tolerance allowed on coupler performance.

Figure 25 contains a compilation of the data obtained. Each point consists of the average of two readings: one reading corresponds to bridge terminals 2' and 3' attached to 2 and 3 on the coupler, respectively, the other corresponds to bridge terminals 2' and 3' attached to 3 and 2 on the coupler, respectively. (See Figure 24.) This averaging removes most remaining uncertainty as to the location of the bridge center.

The data indicates that the phase between output ports is nearly within the 3-degree tolerance relative to the desired 90-degree relationship. It is expected that with greater padding, the bridge would indicate improved performance, although occasional excursions beyond the 3-degree tolerance may exist in the device. The intrinsic performance of the coupler, less connector VSWR, etc., is known to be better than the data contained in Figure 25.



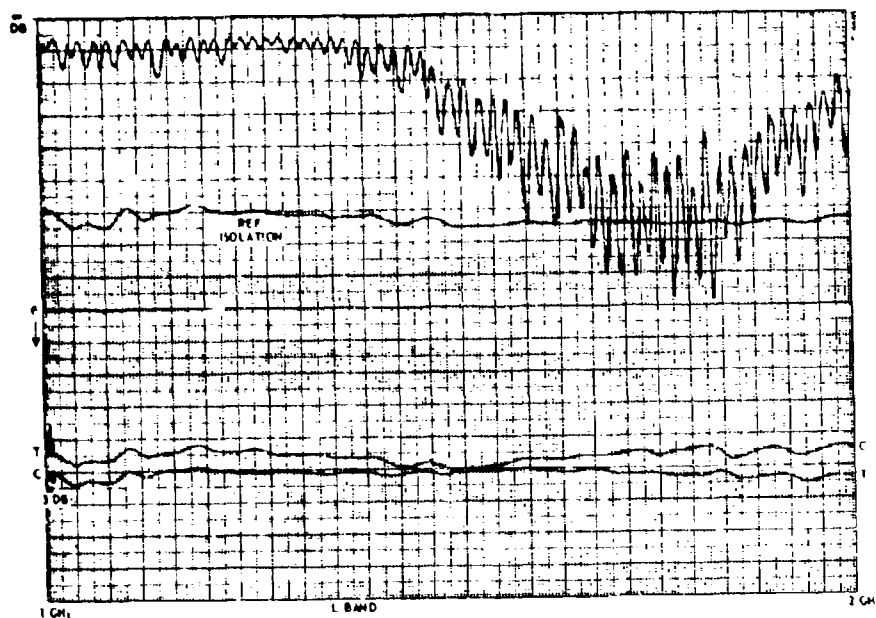


Figure 15 - Isolation, Transmission, and Coupling at L-Band: Input at Port 1

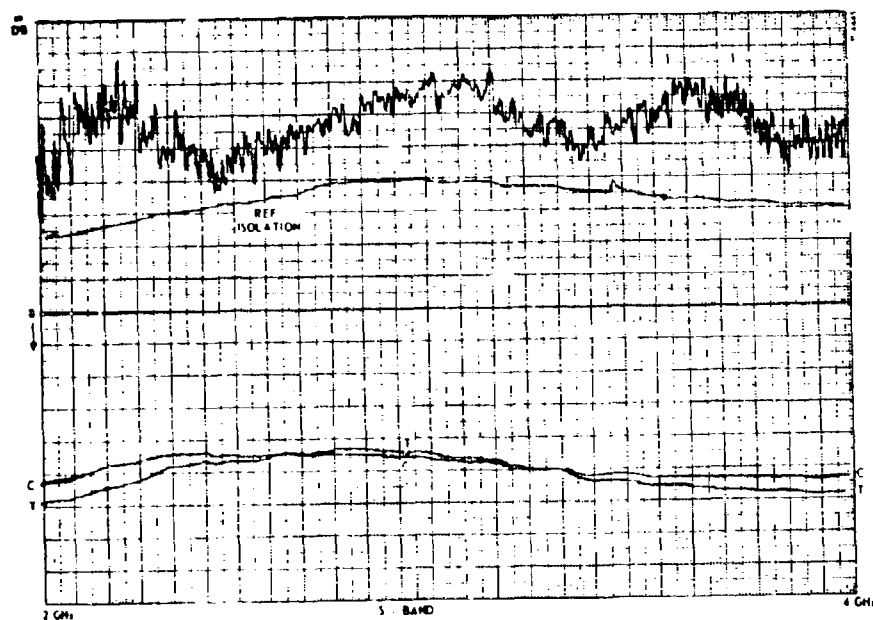


Figure 16 - Isolation, Transmission, and Coupling at S-Band: Input at Port 1

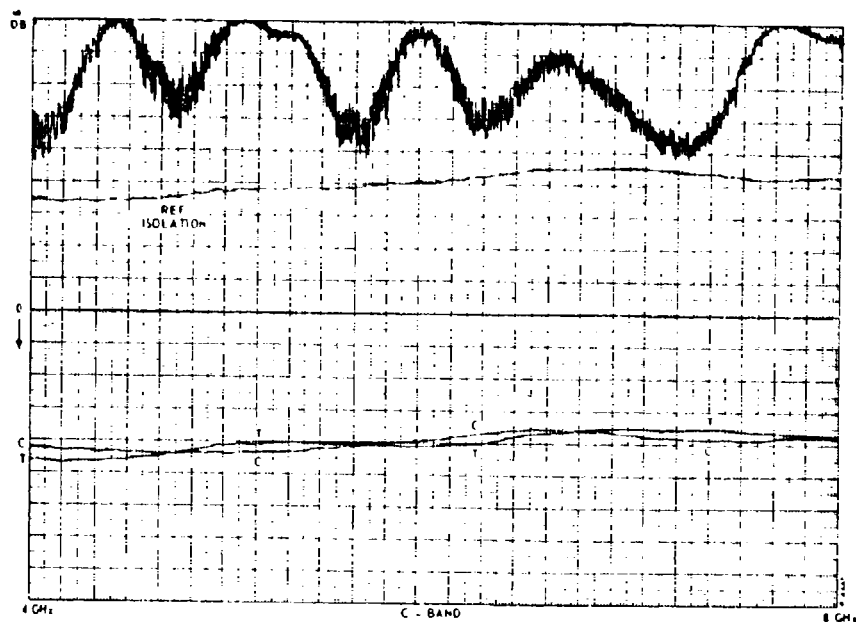


Figure 17 - Isolation, Transmission, and Coupling at C-Band: Input at Port 1

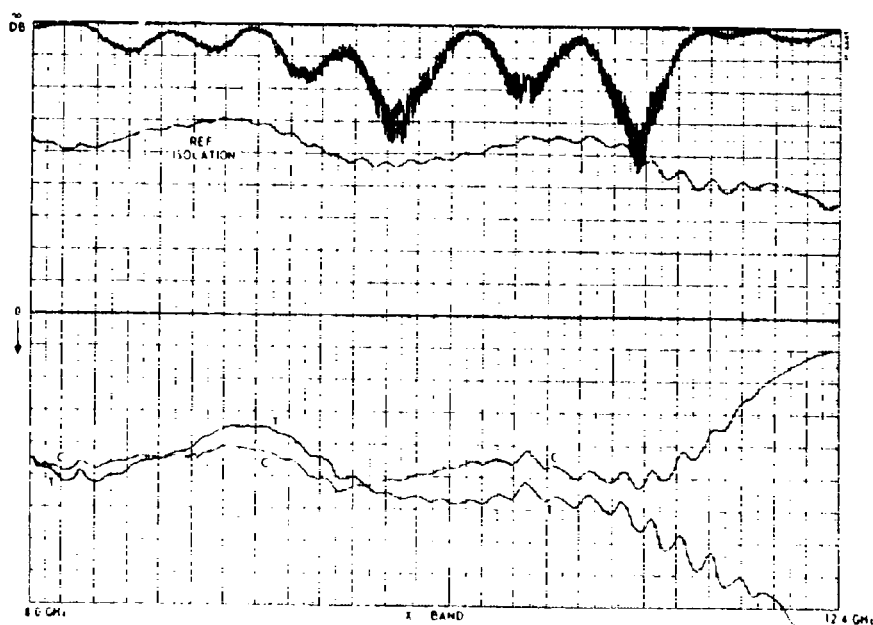


Figure 18 - Isolation, Transmission, and Coupling at X-Band: Input at Port 1

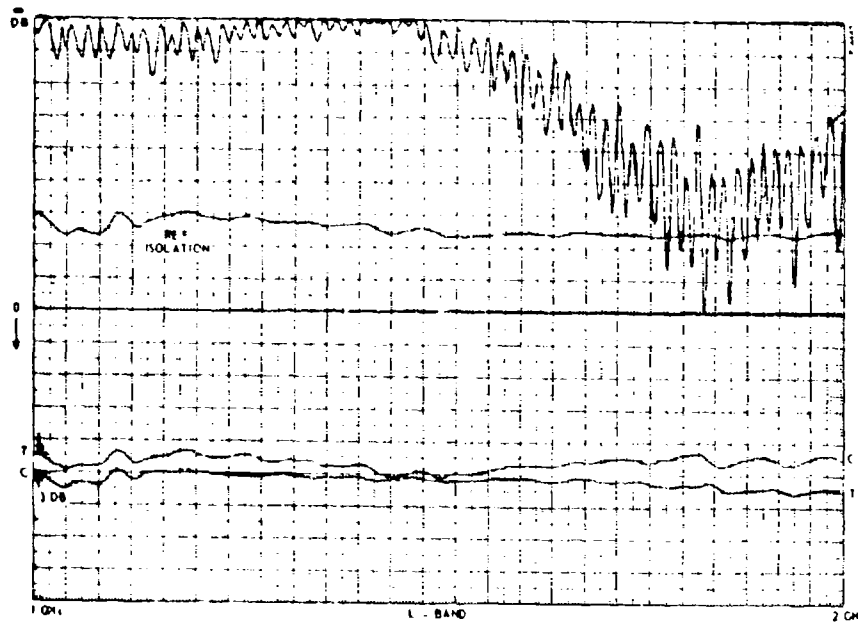


Figure 19 - Isolation, Transmission, and Coupling at L-Band: Input at Port 3

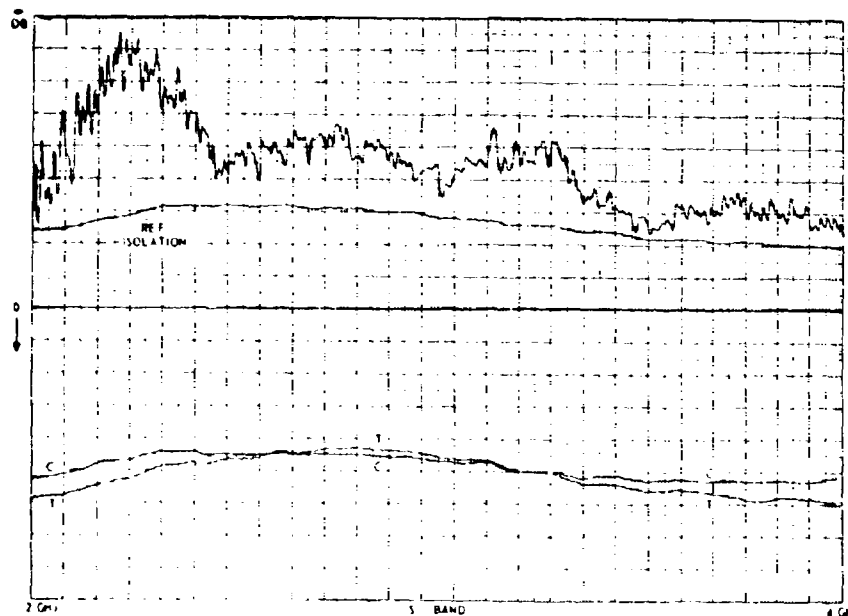


Figure 20 - Isolation, Transmission, and Coupling at S-Band: Input at Port 3

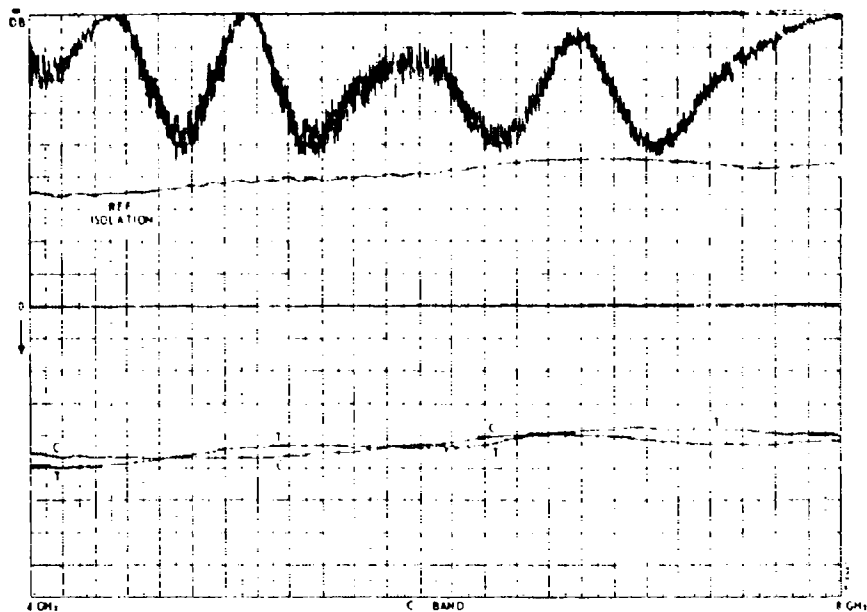


Figure 21 - Isolation, Transmission, and Coupling at C-Band: Input at Port 3

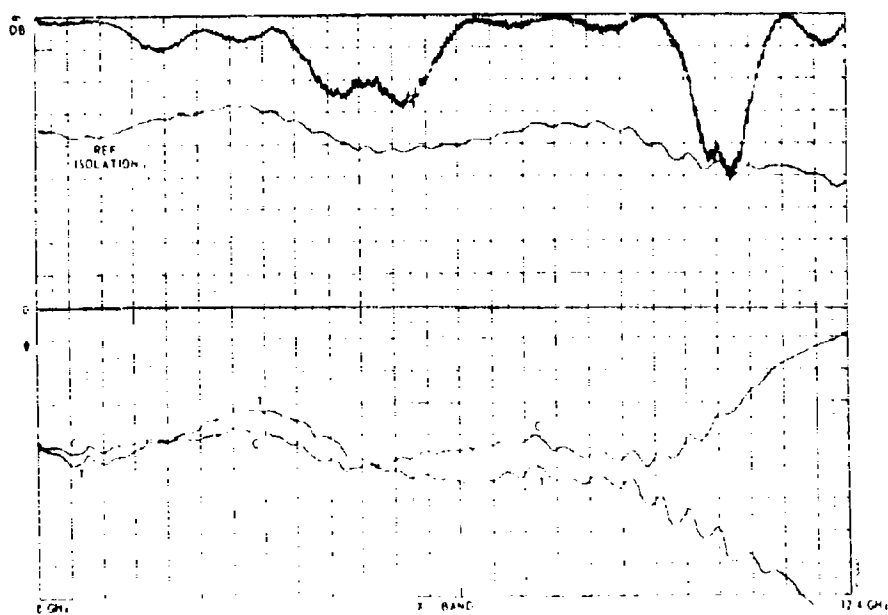


Figure 22 - Isolation, Transmission, and Coupling at X-Band: Input at Port 3

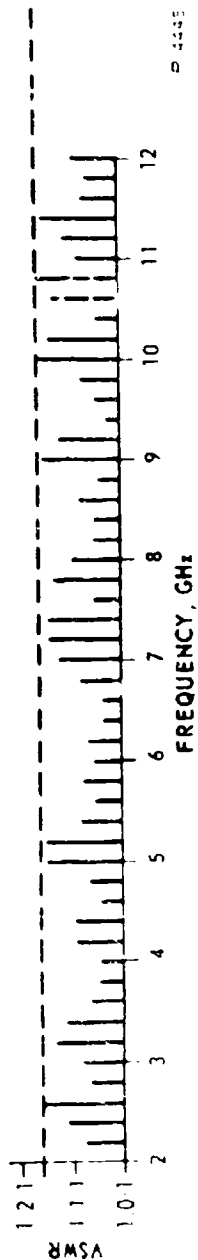


Figure 23 - Coupler VSWR

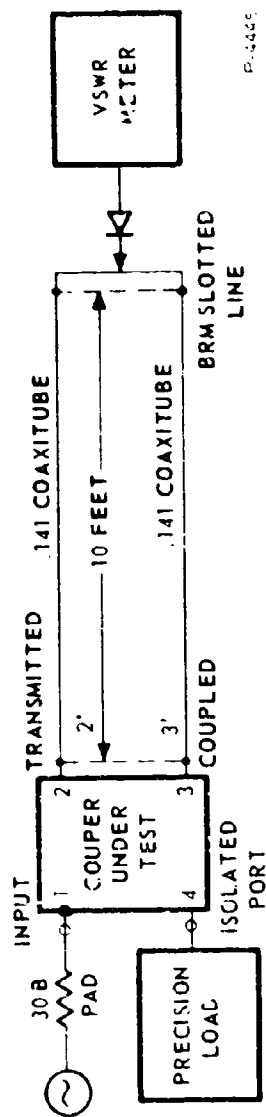


Figure 24 - Final Phase Measurement SetU

NOTE: POSITIVE DEVIATION INDICATES GREATER THAN 90° RELATIVE PHASE LEAD OF COUPLED vs TRANSMITTED SIGNALS

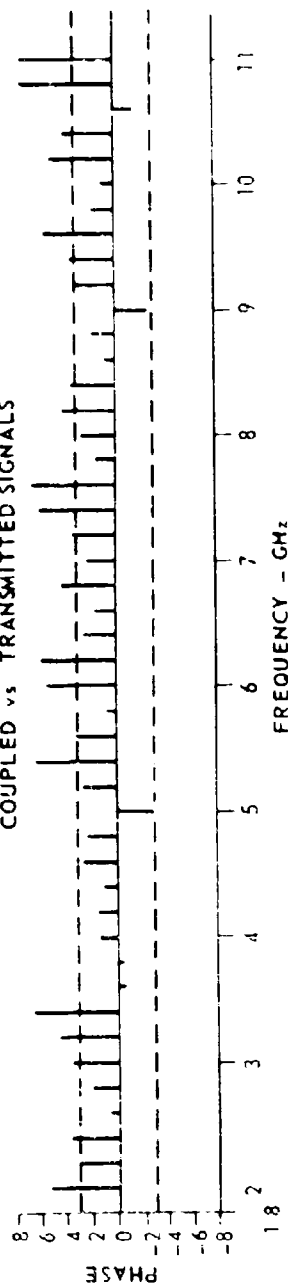


Figure 25 - Phase Deviation of Coupler Outputs from 90°

## SECTION 5

### CONCLUSIONS

The coupler developed on this program meets a majority of the design goals over the 800-11,000 MHz band. Minimum isolation of the delivered model is 23 db, occurring in L-band. Isolation improves with increasing frequency, and is higher than the 25-db specification throughout the X-band region. A second model of the above design exhibited nearly identical performance with a minimum isolation of 24 db in L-band.

The measured VSWR of the coupler is low in keeping with the high isolation characteristic. The average VSWR is approximately 1.09:1 over the band of interest with occasional peaks rising to 1.16:1. The latter value corresponds to the 1.3-db maximum VSWR allowed in the specification. The quoted VSWR values include contributions from the BRM-OSM connectors and from the coax-to-stripline transitions employed. The inherent VSWR of the coupler itself can be expected to be lower and therefore is quite suitable for use in antenna array networks.

Measured insertion loss of the coupler is a maximum of 0.55 db in the vicinity of 11 GHz.

Coupling unbalance of 1 db or less has been met over the band of interest. The initial unmodified design resulted in a slight coupling droop at the high-frequency end of the band. A modified design procedure has been presented which compensates for this droop. This technique, should produce coupling balance well within the 1 db allowed specification. The delivered model, which incorporated a specially designed dielectric shim to correct for this high frequency droop, met the 1-db specification throughout the 800-11,000 MHz band.

The specification on output phase is  $90 \pm 3$  degrees. The measured phase deviation is typically about  $\pm 3$  degrees across the band; the greatest peak deviation measured was  $\pm 8$  degrees. However, bridge setup employed can, under adverse conditions, exhibit inaccuracies of several degrees. Refinement of the measurement requires bridge components that could not be obtained or developed within the time scale of the program.

The present program has proven the value of tapering for the improvement of isolation and the reduction of VSWR in broadband stripline couplers. The resulting design is believed to be the first 90-degree hybrid to exhibit greater than 20-db directivity over the band from UHF to X-band.

A theoretical design which covers the band from 390-11,000 MHz is discussed in the report. The primary limitation in designs having this bandwidth is the insertion loss at high frequencies due to the length of line employed to obtain coupling at low frequencies.

A promising field of investigation would be the extension of coupling into the K-band region. The isolation and VSWR performance of the present coupler are excellent through X-band and into K-band. By changing the frequency scaling, it should prove possible to extend the flat coupling region into K-band while retaining approximately the performance described in this report.

SECTION 6  
REFERENCES

1. E. G. Cristal, L. Young, "Theory and Tables of Optimum Symmetrical TEM Mode Coupled Transmission Line Directional Couplers," IEEE Transactions on Microwave Theory and Techniques, (September 1965), 545-58
2. J. P. Shelton, R. Van Wagoner, and J. J. Wolfe, "Tandem Couplers and Phase Shifters: A New Class of Unlimited Bandwidth Components," Fourteenth Annual Symposium, USAF Antenna Research and Development Program, Air Force Avionics Laboratory, Wright-Patterson Air Force Base, Ohio, in cooperation with the University of Illinois (October 6-8, 1964), Monticello, Illinois, or see Microwaves, April 1965, 14-19
3. C. B. Sharpe, "An Alternative Derivation of Orlov's Synthesis Formula for Nonuniform Lines," Proceedings of the IEE, Part C, Monograph 483E, 109 (1962)
4. D. C. Youla, "Analysis and Synthesis of Arbitrarily Terminated Lossless Nonuniform Lines," IEEE Transactions on Circuit Theory, CT-11, No. 3 (September 1964).
5. R. W. P. King, The Theory of Linear Antennas, Harvard University Press (1956), 857-864.
6. Tables of Sine, Cosine, and Exponential Integrals, Table III. Federal Works Administration, Works Progress Administration, New York (1940).
7. Handbook of Mathematical Functions, U.S. Department of Commerce, National Bureau of Standards, United Mathematics Series 55, U.S. Government Printing Office, Washington, D. C. (June 1964) Chapter 5.
8. Ibid, Table 4.19
9. J. P. Shelton, "Synthesis and Design of Wideband TEM Directional Couplers," presented at International Conference on Microwaves, Circuit Theory, and Information Theory, 10 September 1964, Tokyo, Japan
10. J. P. Shelton, "Impedance of Offset Parallel-Coupled Strip Transmission Lines," IEEE Transactions on Microwave Theory and Techniques (January 1966), 7-15